CONTEXT, CIRCUIT AND MODULATION OF COURTSHIP SIGNAL SELECTION IN *DROSOPHILA*

Dissertation for the award of the degree
Doctor rerum naturalium (Dr. rer. nat.)
of the Georg-August-Universität Göttingen

within the doctoral program Neurosciences
of the Georg-August University School of Science (GAUSS)

submitted by

ELSA STEINFATH
from Darmstadt, Germany

December 2022

THESIS COMMITTEE AND EXAMINATION BOARD MEMBERS

First referee and supervisor
DR. JAN CLEMENS
Neural Computation and Behavior group
European Neuroscience Institute – Göttingen

Second referee
PROF. DR. MARTIN GÖPFERT
Department of Cellular Neurobiology
Schwann-Schleiden Research Centre, University of Göttingen

DR. VIOLA PRIESEMANN
Neural Systems Theory group
Max Planck Institute for Dynamics and Self-Organization, Göttingen

FURTHER MEMBERS OF THE EXAMINATION BOARD

MD, PHD AREZOO POORESMAEILI
Perception and Cognition group
European Neuroscience Institute – Göttingen

PROF. DR. ANDREAS STUMPNER
Department of Cellular Neurobiology
Schwann-Schleiden Research Centre, University of Göttingen

PROF. DR. ANDRÉ FIALA
Department of Molecular Neurobiology of Behaviour
Schwann-Schleiden Research Centre, University of Göttingen

Date of oral examination: February 10, 2023

On the rhythm and rhyme that's designed to
Make your behind move to what I'm inclined to
[...]
I command you to dance
I wanna see motivation
Come on now feel the VIBRATION.

— Marky Mark and the Funky Bunch, 1991

ACKNOWLEDGEMENTS

First and foremost I would like to thank my supervisor Jan Clemens. He was much more than a competent, friendly and supportive supervisor. The way of running his lab in a progressive, open-minded and relaxed manner created a work environment for me to develop skills, personally grow and be creative. He encouraged me to outreach to other researchers, was constantly available for discussion and questions, gave constructive feedback whenever needed, shaped my entire understanding of quantitative research on behavior and reinforced new, sometimes crazy ideas. You know that I really enjoyed doing my PhD in your lab, Jan. I don't take this for granted and it leaves me with deep appreciation and gratitude.

I thank my committee members, Martin Göpfert, Viola Priesemann and formerly Marion Silies for their feedback and suggestions. My gratitude goes also to the neuroscience coordination office, namely Sandra, Jonas and Franziska as well as the ENI staff for their support.
I really enjoyed being part of a *fly team* and thank my lab mates and our technicians past and present: Deniz, Adrian, Melli, Julian, Sarath, Afshin, Daesung, Winston, Dawn, Christine, Kimia and Fred. I am grateful for discussions, joint lunches, fun events, support in all sorts of way and shared moments. Special thanks for major collaboration in this PhD project go to Afshin, Melli and Kimia as well as a number of rotation students and student assistants.

Thanks to my regular climbing partners: Jakob, Max, Max and Max – I love you guys! – and also to my dear friends, amongst them Clara and Caro with Ada. Thanks to my flat mates, namely Knut, Simon and Leandra, who became a second family to me during the pandemic. I thank Tom, my beloved companion in the first half of the PhD. I thank Knut for being my A+ man and the king of the kitchen. I am grateful for the forest and experimental botanical gardens. Their flora, fauna, colors and views grounded me almost every day.

Finally, I thank my family. Thank you, Mama, Papa and Jacob for always having my back, your love, support and encouragement. I share this achievement with you.

ABSTRACT

Communication is multi-modal – when we interact, we speak, gesticulate, and touch. However, the neural computations and circuits that select and coordinate these communication signals are unclear. We address this issue in *Drosophila melanogaster* which, thanks to its complex social behavior and genetic toolbox for manipulating neural activity, is ideal for dissecting the neural basis underlying communication.

The courtship ritual, crucial for the survival of the species, is a social behavior which relies on successful communication between male and female flies. The male fly produces a range of signals based on feedback cues from the female to increase his chance of mating. When close to a female, he extends and vibrates one wing to generate airborne signals, known as the *courtship song*, but also generates *substrate-borne vibrations*, providing an additional communication cue to her. Here, we study the specific behavioral context in which vibration signals are chosen over courtship song. On top of that, we propose a central circuit controlling courtship signal selection and test how the circuit's dynamics are modulated by internal state and sensory cues to support context-dependent signaling in social interactions.

We developed an experimental setup to record the interactions of courting flies alongside the male song and vibrations. Statistical modeling of the flies' pose properties suggests that males vibrate in response to female immobility. We confirm this hypothesis by optogenetically controlling female walking during courtship.

Asking how the selection of courtship signals is centrally controlled, we found two neuron clusters which control vibration and song production with complex dynamics: P1a and pC2l. While optogenetic activation of P1a neurons primarily drives persistent vibrations, pC2l neurons induce song production followed by vibrations. We propose an underlying circuit in which the two clusters drive the output of either signal type while cross inhibiting each other when active. A recurrent network acts presumably on P1a to maintain the persistent vibrations outlasting the neurons activity. This suggests that the two communication modes – song and vibration – are not only controlled by a cross-talk between different neuron clusters but also with distinct temporal dynamics, to provide persuasive communication output of the male.

Lastly, we show that internal state and sensory cues modify the intrinsic circuit dynamics. Sexually satiated males and naive, highly motivated males differ in their internal state. A lower courtship drive reduces signal output of both clusters P1a and pC2l on intermediate time scales. Sensory cues provided by a receptive female quickly overwrite downstream effects of our circuit motif but also reveal that the mutual inhibition between both outputs is agnostic to social cues.

With this, we provide insight into 1) how a social being such as the vinegar fly chooses for a communication signal type depending on its behavioral context and 2) how a neural circuit driving the output of different signal modalities is modulated by internal state and social cues to achieve context-dependent signal selection.

CONTENTS

ACRONYMS

AMMC antennal mechanosensory and motor center

ATP adenosine 5’-triphosphate

cVA *cis*-vaccenyl acetate

DN descending neuron

GLM generalized linear model

HVC high vocal center

IPI inter-pulse interval

LC Lobula columnar

LED light-emitting diode

NPF neuropeptide F

VNC ventral nerve cord

1

INTRODUCTION

1.1 COMMUNICATION IS CRUCIAL AND OFTEN MULTI-MODAL

Throughout the animal kingdom, the generation and perception of communication signals is fundamental for survival and reproduction. Communication plays a crucial role for individuals to find food, avoid predators, resolve conflicts or to select an appropriate mate (Baker, Clemens, and Murthy 2019).

Most species rely on multiple signal types and modalities to provide different kinds of information. Relying on multiple modalities in a defined social interaction, makes the interaction more robust, if one signal channel suffers from noise distortion due to current conditions or in case of limitations on receiver sensory organs (Bradbury and Vehrencamp 2011). Often, depending on context, one signal is more appropriate than another. When seeing a friend from far, we would rather wave our hand whereas we would go for a "hi, how are you" once our friend stands next to us. Just like that, male flies from different *Drosophila* species select a courtship signal depending on the situation. Species with visual signals such as wing or leg displays will present these body parts when in front of a female where she can see them (Yeh, Liou, and True 2006; Setoguchi et al. 2014), whereas courtship song is usually produced when a male is behind a female, chasing her (Coen et al. 2014; Calhoun, Pillow, and Murthy 2019). The courtship song, an acoustic signal, will reach a female even when she walks at varying distance to the male.

Communication signals, depending on species, span chemical, visual, mechanical, electrical, or auditory cues (Baker, Clemens, and Murthy 2019). In mate selection, a variety of different signals and behaviors are woven into a sequence called courtship. These signals provide information about the partner's species, sex, quality and receptivity, and guide synchronization of mating. The ultimate goal of courtship behavior is successful mating but the exchange of a single signal rarely leads to copulation. Instead, animals usually display an elaborate courtship ritual that includes multiple signals and appropriate feedback responses with an ongoing evaluation of the perceived cues (Bradbury and Vehrencamp 2011). The coordination of multiple signals may serve as "honest signals" in sexual selection, informing the partner about physical and mental fitness that cannot be faked. Following this notion, *Drosophila* males demonstrate their fitness by precisely coordinating and timing multiple complex motor elements (Swain and Philipsborn 2021).

1.1.1 *Drosophila courtship signals: song and vibrations*

The courtship ritual of *Drosophila*, crucial for reproduction, is a social behavior which relies on successful communication between male and female flies.

When a sexually mature male fly encounters a female, he displays characteristic courtship behavior. He orients towards the female, follows her, taps her with his forelegs, extends

his proboscis to lick the female and attempts to mount her while bending his abdomen for copulation (Yamamoto and Koganezawa 2013; McKellar et al. 2019). Courtship initiation and pursuit are guided by multiple sensory cues like olfactory and gustatory pheromones or visual input of the moving target (Zhang, Miner, et al. 2018; Kallman, Kim, and Scott 2015; Hindmarsh Sten et al. 2021, see Sensory cues 1.5.1).

The male selects between a range of courtship signals based on feedback cues from the female to increase his chance of mating. A courting male extends and vibrates one wing to generate air-borne signals, known as the courtship song (Shorey 1962) but he also produces substrate-borne vibration pulses in regular trains (Fabre et al. 2012), providing an additional communication cue to her. The male quickly alternates between three song modes (sine, fast pulse and slow pulse song) and flexibly adjusts song bout patterning depending on female feedback (Coen et al. 2014; Clemens et al. 2018; Calhoun, Pillow, and Murthy 2019). He sings pulse trains consisting of short pulses spaced with a species-specific inter-pulse interval (IPI) when chasing the female. The two pulse modes (fast and slow) are distinguished based on their carrier frequency and waveform symmetry. Fast pulse song consists of an asymmetric waveform with faster oscillations (250-400Hz) than slow pulse song, which is symmetrical and shows slower frequencies (200-250Hz, Clemens et al. 2018). The male produces the louder fast pulse song when he is far from the female and the softer slow pulse song when closer (Clemens et al. 2018; Calhoun, Pillow, and Murthy 2019). The soft sine song, a humming sound at around 160 Hz, is sung by the male when very near to the female (Coen et al. 2014; Clemens et al. 2018). Detailed behavioral tracking combined with advanced statistical modeling revealed that it is in fact both, the male's sensorimotor strategies and female behavioral cues, that govern song type selection (Calhoun, Pillow, and Murthy 2019).

Set-ups to record fly communication are usually equipped with microphones, therefore the air-borne courtship song is picked up easily and could be described in such detail since its discovery (Shorey 1962). Substrate-borne vibrations on the other hand, are harder to detect and have been hardly studied until now in *Drosophila melanogaster* (Fabre et al. 2012; Mazzoni, Anfora, and Virant-Doberlet 2013, other *Drosophila* species: Hernández and Fabre 2016). This is surprising, as vibration communication is extremely common and important in the insect kingdom (reviewed in Hill 2001; Cocroft and Rodríguez 2005; Stritih-Peljhan and Virant-Doberlet 2021). *Drosophila* vibrations classify as tremulation, as they are produced by specific body(-part) movements without striking the substrate (Stritih-Peljhan and Virant-Doberlet 2021). Tremulations are commonly displayed by males during short- as well as long-range courtship also in other species, such as crickets (Broder et al. 2021) or katydids (Morris and Luca 1998). *Drosophila* vibrations come in trains of pulses, with each pulse lasting about 5 ms and an inter-pulse interval of 160 - 250 ms (Fabre et al. 2012; McKelvey et al. 2021). Male vibrations are associated with female immobility (Fabre et al. 2012; McKelvey et al. 2021), suggesting that behavioral context plays a role for their selection, just like it does for song.

The *Drosophila* courtship ritual provides an excellent model to study social behavior. In recent years tools for pose tracking (Graving et al. 2019; Pereira et al. 2019; Mathis et al. 2018) and automated audio annotation (Steinfath et al. 2021; Cohen et al. 2022; Coffey, Marx, and Neumaier 2019) have been developed to a level which allows to quantify

animal's behavior with large and detailed data sets. This gives us the opportunity to describe how animals shape their behavior in a natural context instead of training animals on artificial tasks. *Drosophila* brains and behavior are at the sweet spot of complexity with a versatile but also limited repertoire of neurons and actions, facilitating to break down brain processes, circuits or behavioral composition into models. In *Drosophila* such models can often be tested directly. Genetic access to neurons or neuron clusters (Luan et al. 2006; Golic and Lindquist 1989; Brand and Perrimon 1993), combined with genetic tools, offers a broad range of precise manipulations which are not possible in any other model organism today. With optogenetic tools, for example, we can inhibit (Mauss, Busch, and Borst 2017) or activate (Klapoetke et al. 2014) selected neurons at any given moment in time and flexibly adjust duration and intensity of neuronal in-/activity. By combining behavioral quantification and optogenetics, we can even take it one step further and study neuronal control during natural behavior. In this study we make use of these opportunities and study neural control of signal production and neural processes underlying signal selection in *Drosophila* courtship behavior.

1.2 SIGNAL PERCEPTION AND RESPONSE

1.2.1 *Female signal recognition*

Communication involves at least two: a sender and a receiver. In the case of *Drosophila* courtship signals, the intended receiver is the courted female. Females pick up the male's courtship song with their arista. This feathery bristle at the tip of the antenna deflects with air particle velocity fluctuation (Göpfert and Robert 2002) and subsequently excites the Johnston organ neurons (Ewing 1978). These mechanosensory neurons mainly project from the antenna to the antennal mechanosensory and motor center (AMMC) (Kamikouchi, Shimada, and Ito 2006; Patella and Wilson 2018), where they connect to secondary neurons which pass the information to higher brain areas, like the wedge (Patella and Wilson 2018). Brain wide imaging in the female brain revealed that neurons responding to the courtship song modes sine and pulse lie in areas throughout the entire central brain (Pacheco et al. 2021). Processing centers, higher in the auditory pathway than the AMMC, become more selective for courtship song signals, while most regions are tuned to either pulse or sine song. The selectivity for the different song modes arises in neurons directly downstream of the Johnstons organ neurons (Baker, McKellar, et al. 2022). Narrow pulse-song tuning could be pinpointed to the sex-specific neurons pC2l but also the *doublesex* positive clusters pC1 and MN2 (Deutsch et al. 2019), MN2 is female-specific (Kimura et al. 2015). In fact, a number of higher-order auditory neurons in the wedge and the ventrolateral protocerebrum show clear sine or pulse preferences. They form a highly interconnected network and send projections throughout the brain (Baker, McKellar, et al. 2022).

Vibration signals were recently shown to be picked up with mechanosensory neurons in female legs (McKelvey et al. 2021). The femoral chordotonal organ is proprioceptive and lies within the femur of a fly's leg (Field and Matheson 1998). Subtypes of femoral chordotonal organ neurons encode different features of leg movement, including vibra-

tional deflections in frequencies that match the male's vibration signals (Mamiya, Gurung, and Tuthill 2018). Some femoral chordotonal organ neurons project directly to the gnathal ganglia, wedge and ventral anterior ventrolateral protocerebrum (Tsubouchi et al. 2017), others via secondary neurons (Agrawal et al. 2020). However, how courtship vibrations are processed centrally has not been investigated yet.

1.2.2 *Signs of female receptivity*

While the courtship efforts of a male fly are easily detectable for the human eye, a female's signs of receptivity are more subtle. Slower walking, even stopping (Markow and Hanson 1981; Bussell et al. 2014) and abdominal grooming (Lasbleiz, Ferveur, and Everaerts 2006) in response to a male's courtship pursuit indicate her receptivity. However, for final acceptance the female will open her vaginal plates (Kimura et al. 2015; Wang et al. 2021; Mezzera et al. 2020; Duckhorn et al. 2022) and allow copulation. Therefore copulation latencies and frequencies are common measures of courtship success.

Courtship song highly contributes to mating success, as deaf females or females courted by a wing-cut male rarely copulate (Coen et al. 2014). The mating success of a wing-cut male can be restored by pulse song playback (Yamada et al. 2018; Li, Ishimoto, and Kamikouchi 2018; Bennet-Clark and Ewing 1969). Receptive females slow down in response to song and the slowing is even tuned to spectrotemporal features of pulse song (Deutsch et al. 2019). A female's final sign of acceptance, the vaginal plate opening is usually preceded by male wing extension (Wang et al. 2021) and a successful copulation attempt is preceded by pulse song (Roemschied et al. 2021), indicating that males and females coordinate the timing of their courtship behaviors.

Vibration signals were argued to promote female immobility (Fabre et al. 2012; McKelvey et al. 2021). When asking by which molecular mechanism females pick up vibrations, two cation channels seem to play a role: Nanchung and Piezo. Both are involved in mechanosensory transduction and expressed in femoral chordotonal organ neurons (Kim et al. 2003; Ramdya et al. 2015). Knockdown of Nanchung in female's femoral chordotonal organ reduces the mating success of a vibrating male (McKelvey et al. 2021).

1.3 NEURAL CONTROL OF SIGNAL PRODUCTION

When wondering how a signal is produced, an intuitive way to start would be to investigate which body part generates it. This body part is moved by muscles that are innervated by motor neurons. For rhythmic activity, central pattern generators add a level of oscillatory control. Upstream of motor neurons and pattern generators lie descending neurons (DNs) which link central command centers to the execution level of motor control. Central circuits select an action based on sensory cues or context. These levels of control are conserved across taxa, which will be examplified for *Drosophila*, mammals and birds in this section.

In *Drosophila*, courtship song is generated by wing movement (Yamamoto and Koganezawa 2013). In mammals, moving lips, jaw and tongue are indicative for vocalizations, although

the vocal fold and respiratory system are not directly visible. In birds, the syrinx and trachea are the vocal organs, acting jointly with tongue, jaw and the rest of the respiratory system (Bolhuis, Okanoya, and Scharff 2010). In all cases, multiple muscles are involved orchestrating the movements of the signal eliciting body parts. Each muscle is innervated by motor neurons. Their timing and activation strength will compose the full motor program required for signal generation. But to achieve fly courtship song with pulse trains at a defined inter-pulse interval or sine song at a fixed frequency, the movement needs to continue rhythmically, here central pattern generators come into play. Central pattern generators generate ongoing and stereotyped movements required for wing fluttering but also for respiratory rhythms which are crucial for mammal or bird vocalizations (Marder and Calabrese 1996; Clyne and Miesenböck 2008; Jürgens 1994; Bolhuis, Okanoya, and Scharff 2010).

For vocalizations in birds and mammals, respiratory rhythms as well as motor coordination and output are all controlled in nuclei of the brain stem (Bolhuis, Okanoya, and Scharff 2010; Jürgens 1994). In flies, motor neurons and pattern generators for wing movement lie in the ventral nerve cord (VNC). Upstream, descending neurons pass the behavioral command from the central brain to the VNC (Namiki et al. 2018).

In flies, descending neurons are controlled by central neurons, which are in the prime spot to collect sensory input providing information on social context, integrate them and determine an appropriate behavioral output. In mammals, the midbrain periaqueductal gray serves as a collector or relay station for the descending vocalization-controlling pathways, it integrates incoming information and triggers specific innate vocal patterns. Artificial activation of periaqueductal gray elicits vocalizations in several species (Jürgens 1994; Bolhuis, Okanoya, and Scharff 2010; Hahnloser, Kozhevnikov, and Fee 2002; Tschida et al. 2019). The bird song motor pathway arises in the forebrain from neurons in the high vocal center (HVC) that project directly to the robust nucleus of the arcopallium. From there the song motor output projects to the brain stem nuclei. Defined neuron populations in the HVC control bird song patterning and tempo (Hahnloser, Kozhevnikov, and Fee 2002; Mooney 2000; Mooney and Prather 2005; Solis and Perkel 2005).

1.3.1 *Central control of Drosophila courtship signal production*

The central circuit underlying song production in *Drosophila melanogaster* is well established: higher order processing centers in the male integrate sensory input to form a courtship decision. These higher neurons then serve as command centers which initiate courtship behavior like singing by driving descending neurons but also maintain a courtship arousal state in the absence of sensory cues by activating persistence nodes. Descending neurons relay the behavioral command from the brain to the ventral nerve cord and serve as a bottle neck for the execution of behaviours (Cande et al. 2018).

As courtship song production is a male exclusive behavior, many neurons for song control are sexually dimorphic or even male-specific. Two major sex determination genes, *fruitless* and *doublesex*, regulate sexual dimorphism in the male and female nervous system during development (Cachero, Ostrovsky, et al. 2010; Yamamoto and Koganezawa

2013; Yu et al. 2010). The higher order courtship neurons pC2l and P1a belong both to the *doublesex* cluster, while P1a is additionally *fruitless* positive.

pC2l neurons respond to visual and auditory courtship cues (Kohatsu and Yamamoto 2015; Deutsch et al. 2019) and drive mainly pulse but also sine song production in males (Deutsch et al. 2019; Roemschied et al. 2021). Pulse and sine output controlled by pC2l follows a stereotypical sequence with pulse song production during pC2l activity, followed by sine production at the offset of pC2l activity. The amount of sine song at the offset scales with duration of optogenetic activation, hinting on dynamics downstream of pC2l that are intrinsic to the courtship song patterning circuit (Roemschied et al. 2021).

P1a is a central neuron cluster which mediates social arousal (Clowney et al. 2015; Hoopfer et al. 2015). P1a integrates information from volatile and contact pheromones (Kohatsu, Koganezawa, and Yamamoto 2011; Clowney et al. 2015; Kallman, Kim, and Scott 2015). Depending on external cues or level of activation P1a drives either aggressive or courtship behavior in male flies (Hoopfer et al. 2015; Jung et al. 2020). Artificial P1a activation gives rise to probabilistic song bouts (Clemens et al. 2018; Roemschied et al. 2021) or wing extensions (Inagaki et al. 2014; Hoopfer et al. 2015; Jung et al. 2020), as consequence of an increased courtship arousal.

P1a induces the maintenance of a social arousal state by activating pCd, a Fru and Dsx expressing neuron cluster which recruits dopaminergic neurons and a central cluster that produces the neuropeptide F (NPF). Together, they can sustain a male's courtship arousal for minutes and even days (Jung et al. 2020; Zhang, Rogulja, and Crickmore 2019; Zhang, Miner, et al. 2018, see Internal states 1.5.2).

P1a was postulated to be upstream of the *fruitless* positive descending neuron pIP10 (Philipsborn et al. 2011). pC2l directly synapses on to pIP10, herby controlling song output (Roemschied et al. 2021; Lillvis et al. 2022). pIP10 relays a courtship song command from the central brain to the wing neuropil in the mesothoracic ganglia of the ventral nerve cord where it activates pattern generators and motor neurons (Philipsborn et al. 2011; Ding et al. 2019). Other than pIP10, one more descending interneurons has been described to drive wing extension and tapping behavior: P2b. However, P2b has been identified using mosaic expression techniques in *fruitless* positive cells (Kohatsu, Koganezawa, and Yamamoto 2011) and in contrast to the previously mentioned neurons, no genetic driver is available.

Between descending neurons and motor neurons lie a set of male-specific song interneurons: vPR6, dPR1 and TN1. All of them are located in the VNC and express *fruitless* and *doublesex* (Philipsborn et al. 2011; Shirangi et al. 2016). In a solitary male dPR1 and vPR6 elicit pulse song whereas TN1A elicits sine song. pIP10 and TN1 were recently suggested to form a circuit motif which, depending on intrinsic connectivity and computations in combination with sensory history, enables context-dependent song patterning (Roemschied et al. 2021).

Whereas the song circuit has been described on several levels, vibration production has been linked to both broad neuron populations controlling courtship behavior: *fruitless* and *doublesex* (Fabre et al. 2012). However, narrower neuron clusters driving vibrations have not been been specified yet. The control of song and vibration production

could either be coordinated in overlapping central circuits and be split on the level of the ventral nerve cord or driven by distinct central circuits.

1.4 ACTION SELECTION: CIRCUITS AND THEIR DYNAMICS

Action selection is the task of choosing "what to do next" from a set of competing behavioural alternatives (Prescott 2008). In this sense, a courting male needs to select from several available actions, for example between courtship signals.

Action selection involves at least three levels. First, an internal state will govern the overall condition of the fly: deciding between sleep, foraging, social interaction or flying for instance. Second, within such a state, external stimuli will specify the behavioral context the fly is in, for example male pheromones will bias the social behavior of a male fly towards aggression whereas female pheromones will promote courtship. Third, once the social context is clear, a defined action (here signal production) needs to be selected from the behavioral repertoire on a moment-to-moment basis (Anderson 2016).

Looking at *Drosophila* courtship signal selection as a specific case of action selection, we can map the different levels of action selection to their neural correlates. The neuron cluster pCd represents internal state neurons. In a recurrent excitation loop with NPF, linked to a dopaminergic system, they store mating drive for minutes up to days and classify as social motivation node (Zhang, Rogulja, and Crickmore 2016; Zhang, Rogulja, and Crickmore 2019; Jung et al. 2020).

Clusters like P1a or pC2l collect sensory evidence informing about social context. Their activity is modulated by both, male and female cues (Kallman, Kim, and Scott 2015; Clowney et al. 2015; Deutsch et al. 2019; Kohatsu and Yamamoto 2015).

P1a drives not only courtship behavior but also aggression, gating behavioral output depending on context. This observation is in line with the idea that in action selection, behaviors are usually not controlled by independent and discrete systems, but rather by neurons that participate in more than one behavior, or differently in a given behavior depending on behavioral demand (Kupfermann and Weiss 2001).

P1a and pC2l are both song pre-command neurons, driving defined actions via descending neurons, like pIP10 or P2b. These descending neurons can be regarded as the bottleneck for behavioral output.

Central circuit motifs for action selection have been postulated and described before (Machens, Romo, and Brody 2005; Wang 2008; Roach, Churchland, and Engel 2022). At their core, most models propose that choice alternatives are represented by pools of recurrently connected excitatory neurons, which compete via inhibitory connectivity (Kuan et al. 2022). Selective neuronal activity within such a circuit will come along with intrinsic circuit dynamics. Driving one node in the circuit will favor a specific action whereas another node will favor the alternative action. Inhibition between two competing nodes will suppress simultaneous output of incompatible actions. To maintain an action output, recurrent connectivity can induce persistent activity of a particular output node.

Considering more complex scenarios, hierarchy in connectivity can result in subsequent activation of nodes which in turn can drive stereotyped sequences of behavioral output (bird song: Long, Jin, and Fee 2010, fly grooming: Seeds et al. 2014). However, such sequential actions can also be achieved by threshold-based ordering (McKellar et al. 2019).

Together with connectivity, intrinsic properties of circuit nodes result in intrinsic circuit dynamics. A classic example is the post-inhibitory rebound, here the connection of an inhibitory input to a circuit node triggers at inhibition offset hyperpolarization-activated cation currents within the node (Angstadt et al. 2005). After inhibition follows then a rebound activity of the node. Another possibility is that a cell can physiologically function as an integrator (Jung et al. 2020). By sustaining its activity is may serve as a memory in the circuit.

The anatomical connectivity within an action selection circuit can be considered as fixed, on timescales relevant for behavior (Battaglia et al. 2012). But for a signal to be context-appropriate, external cues and internal state need to acutely inform signal choice. For example, when extremely hungry it may be beneficial to search for food instead of engaging in a conversation and once fed, the way of talking will depend on the person in front of us and the way it reacts to us. Therefore intrinsic dynamics of the signal selecting motif should be modulated by cues and state. But how sensory context flexibly controls neural circuit activity to guide behavior is, to our knowledge, not understood mechanistically in any system.

1.5 CONTEXT APPROPRIATE SIGNAL SELECTION: SENSORY CUES AND INTERNAL STATE

Selecting the appropriate signal at the right moment will be crucial to get one's message across. A visual signal will only be seen when the receiver is facing in one's direction, for instance. Also it will be beneficial to choose a louder signal when far from one's target and a softer when close. Courting males choose the louder pulse song when they are far away from the female, the softer pulse song when closer and the soft sine song when very near to the female (Coen et al. 2014; Clemens et al. 2018; Calhoun, Pillow, and Murthy 2019). Moreover, the female will show signs of receptivity when the male's song patterning is context-appropriate. She slows down, allowing the male to come closer, only when the male sings the loud, fast pulse song far from her. And a disrupted song mode choice reduces a male's mating success (Clemens et al. 2018). Accordingly, a male fly needs to be informed about the current behavioral context in order to select a signal for production. This behavioral context is encoded by sensory cues as well as internal state of the fly.

1.5.1 *Sensory cues inform about present conditions*

Sensory cues inform about present conditions with different sensory modalities providing different information. For example, in the moment that a male taps a female, he will receive gustatory input from her cuticular pheromones. Contact pheromones are sampled by gustatory receptors on the male's forelegs (Clowney et al. 2015; Kallman, Kim,

and Scott 2015). Not only males and females but also closely related *Drosophila* species express a distinct cuticular pheromone profile (Seeholzer et al. 2018). Hence, from gustatory cues he can extract information about the female's species, sex and even location, since he will only reach her with his foreleg when she is close. The volatile pheromone *cis*-vaccenyl acetate (cVA) is male-specific but also synthesized by males and transferred to a female during copulation, making her unattractive to other males (Clowney et al. 2015; Kurtovic, Widmer, and Dickson 2007; Brieger and Butterworth 1970). Accordingly, cVA functions as an olfactory cue informing about sex or mating status of the encountered fly. On top of that, cVA has been suggested to serve as information source about proximity and relative position of another fly (Taisz et al. 2022).

Visual cues provide the male with location information but also reveal the target's movement and orientation. Lobula columnar (LC) neurons are higher visual projection neurons with distinct functional roles, often conveying courtship-relevant visual information. A number of LC neurons coordinate spatial and/or temporal aspects of the male courtship ritual and support proper positioning of the male relative to female (McKinney and Ben-Shahar 2019). Another particular type, LC10 neurons, preferentially responds to small moving objects, like a female in courtship and guide a male's courtship pursuit (Ribeiro et al. 2018). The sensory gain of LC10 neurons is tuned by courtship arousal. Courtship arousal boosts LC10 responses to a moving target and subsequently enhances the male's ability to track a female more closely (Hindmarsh Sten et al. 2021).

Acoustic cues in courtship arise not only from a male's courtship song but also from motion sounds generated by a walking fly. Such acoustic stimuli generated by movement stimulate courtship initiation in males and are detected by mechanosensory neurons (Ejima and Griffith 2008). Mechanosensors in the fly ear pickup courtship song which also increases a male's social arousal and walking speed, presumably because such a cue suggests that close to him another male courts a receptive female (Deutsch et al. 2019; Li, Ishimoto, and Kamikouchi 2018; Zhou et al. 2015; Yoon et al. 2013).

Together, gustatory, olfactory, visual and acoustic cues dynamically form the sensory experience of a courting male. Combined they guide him in various aspects of the courtship ritual, such as initiation, maintenance, pursuit, positioning and even sensorymotor transformations, because sensory cues shape his understanding of the present context.

1.5.2 *Internal states integrate cue and behavioral history*

Internal states integrate cue and behavioral history. Internal states are processes that underlie the dynamics of a nervous system. They broadly effect behavior and systemic physiology by influencing neural activity and neuromodulation (Flavell et al. 2022). They support the evaluation of competing drives on a higher level, for example between feeding, sleeping or reproductive behaviors. In courtship, internal states set short term arousal and long term motivation.

The internal state of social arousal can manifest in a male's courtship drive for instance. His courtship drive depends on sexual experience. Once he has mated successfully a number of times, it will be less likely that he initiates or maintains courtship

towards another receptive female (Zhang, Rogulja, and Crickmore 2019). Accordingly, depending on behavioral history, a change in internal state, here courtship motivation, changes a male's behavior. Courtship drive is regulated on at least two timescales in *Drosophila*: on an arousal level of minutes and a motivation level of hours or days.

The neural processes controlling both levels of courtship drive are well understood. P1a acutely promotes social behaviors like courtship or aggression but it also induces an internal state of social arousal lasting for several minutes (Jung et al. 2020; Hoopfer et al. 2015). Although P1a neurons induce this state, P1a activity decays quickly with time, pointing to downstream neurons encoding the state of social arousal (Hoopfer et al. 2015; Inagaki et al. 2014). pCd neurons sustain persistent activity in response to P1a activation (Jung et al. 2020). This persistent pCd activity is required for the maintenance of courtship and aggressive behaviors following P1a activation and may be regarded as a working memory of P1a activity. Although pCd amplifies social behaviors, its activity is not sufficient to induce them but requires additional activity of P1a (Jung et al. 2020).

On longer timescales of days, a recurrent connection of pCd and NPF-expressing cells build up courtship motivation if males do not copulate (Zhang, Rogulja, and Crickmore 2019). This recurrent circuit promotes courtship by increasing P1 (of which P1a is a subgroup) activity via dopaminergic neurons. Enhanced dopaminergic activity in the superior medial protocerebrum additionally de-sensitizes the P1 response to inhibition (Zhang, Rogulja, and Crickmore 2019; Zhang, Miner, et al. 2018).

Sexual satiety is induced by a group of copulation reporting neurons in the abdominal ganglion. They project from the genitalia to the brain and inhibit NPF neurons, herby reducing courtship drive (Zhang, Rogulja, and Crickmore 2019). Males recover from sexual satiety by a gradual increase in the excitability of the recurrent circuit comprising pCd and NPF (Zhang, Rogulja, and Crickmore 2019).

Courtship drive competes with other needs such as feeding or sleeping. P1a functions as a neural node mediating between courtship drive and other innate behaviors (Jiang and Pan 2022). Reciprocal inhibition between sex and sleep circuits regulates the choice between courtship and sleep. Enhanced mating drive, in naive males or artificially maintained by P1a activation, suppresses sleep for hours via octopaminergic neurons (Machado et al. 2017). In contrast sleep deprivation reduces the intensity of male courtship by decreased P1a activity (Chen, Sitaraman, et al. 2017). Whereas sleep and courtship are incompatible actions, feeding and courtship are not necessarily. The preference for sex versus feeding relies on the urgency of either need as well as the quality of present resources (food and potential mates). When a starved male is simultaneously presented with a potential mate and food, he usually initiates feeding first but reverses the choice after a few minutes and switches to courtship. It is again P1a encoding a high courtship arousal, acutely decreasing feeding in starved males (Cheriyamkunnel et al. 2021).

These findings suggest that P1a neurons induce a social arousal state on short time scales and are a target of state-dependent modulation in males with high courtship motivation on longer time scales (Devineni and Scaplen 2022). Together with social cues, the internal state of a male defines his behavioral context. Internal states govern on intermediate and longer time scales if a behavior is initiated and maintained. Sensory

cues refine and update the internal representation of the current context and guide selection of actions on moment-to-moment basis.

1.6 THESIS OVERVIEW AND OBJECTIVES

Communication is crucial for many animals to survive and reproduce. We have a good understanding of how a communication signal is produced in different taxa like mammals, birds and insects – from central brain areas controlling their output to muscles and body parts generating them. The central circuits underlying signal production are anatomically fixed, on timescales relevant for behavior. From the connectivity between and the properties within circuit nodes result intrinsic dynamics that can give rise to complex signal sequences. However, for successful communication most animals do not produce a stereotypic signal sequence but select between different signals depending on context. Accordingly, the intrinsic dynamics of selecting circuits should be adaptive to external cues and internal state defining the current context.

With *Drosophila melanogaster* we have an excellent model system that engages in diverse social behaviors, like an elaborate courtship ritual and elicits a number of signals with different modalities. Because of genetic access to neuron clusters, we have now the possibility to study circuits controlling signal selection in the fly brain and probe them for modulation by social cues or changes in internal state.

Therefore, the aim of this thesis was to 1) quantify the behavioral context in which the male produces two distinct courtship signals: song and vibrations, 2) identify a brain circuit driving the two different communication signals and 3) test how social cues as well as internal state modulate the output of this circuit.

In Section 3.1 we establish a set-up to record both signal modalities in fly courtship: air-borne courtship song and substrate-borne vibrations and simultaneously track the behavior of the flies. We use these data to describe differences between the signal types but also the properties of vibration signals which are less well studied than song.

In the following Section 3.2 we show that the selection between these signals is context-dependent. We turn to generalized linear models (GLMs) to define which behavioral cues are important for the male to select between signals and pinpoint in which way the different cues inform his choice. We find that males sing when close to the female and that they vibrate when the female as well as himself are immobile. We confirm the model behaviorally: by controlling female speed we show that female immobility is a necessary and sufficient trigger for the male to engage in vibration behavior.

Next (Section 3.3) we set out to identify which brain circuits underlie the male's communication. We introduce two central neuron clusters – pC2l and P1a – which preferentially drive one of the courtship signals: song and vibrations respectively. However, their output dynamics are more complex and yield a signal sequence in case of pC2l and a persistent, rather probabilistic output of both signal types in case of P1a. From this we infer a circuit motif which orchestrates signal selection centrally. Initially, we optogenetically drive parts of the circuit in solitary males and describe the behavior resulting

from intrinsic circuit dynamics. Afterwards (Section 3.4), we reduce courtship drive in the males, to test how a change in internal state will effect the circuits dynamics. Finally (Section 3.5), we provide social cues in addition to neuron activation, to test which aspects of the intrinsic dynamics will be modulated by socials cues.

We find that a lower courtship drive reduces the overall signal output of the circuit, regardless of the neuron cluster we drive and that the output is affected at intermediate time scales. When providing social cues by introducing the males to a female, we find that the neurons still yield their respective signal output during stimulation, whereas the dynamics we observe after stimulation are quickly modulated by social cues and level back to baseline. Furthermore, the exposure to social cues reveals that a mutual inhibition between both signal outputs is agnostic to social cues.

Thus, the contributions of this thesis are threefold: we quantitatively describe the properties and context of vibration signals in relation to courtship song, propose a central circuit motif which orchestrates their output and study how this circuit is modulated by internal state and sensory cues to enable context-dependent communication.

2

MATERIAL AND METHODS

2.1 FLY STRAINS AND REARING

Flies were kept on a 12:12-h dark:light cycle, at 25°C and 60% humidity. Flies were housed in groups of 3-15 flies of the same sex.

Table 1: Fly lines.

FIGURE	NAME	GENOTYPE	SOURCE	PROVIDED BY
1-2.1,7	wild-type	*Drosophila melanogaster* NM91	Coen et al. 2014	Peter Andolfatto
1.1	wild-type	*Drosophila melanogaster* OregonR		
2	vGlut	vGlut-OK371-Gal4 x UAS20x-GtACR1 (III)	Mauss, Busch, and Borst 2017	vGlut by Martin Göpfert
2	DNp28	R11H10-p65ADZp (II); VT033947-ZpGdbd (III) x UAS20x-CsChrimson	Bidaye et al. 2020; Klapoetke et al. 2014	DNp28 (SS01587) by Gwyneth Card, CsChrimson by André Fiala
2-7	pC2l	UAS<stop>CsChrimson.mVenus/s (II); LexAop-FLP,dsx-LexA/R42B01 Gal4 (III)	Deutsch et al. 2019	Vivek Jayaraman
4-7	P1a	UAS20x-CsChrimson.mVenus (II) x R15A01.AD;R71G01.DBD	Hoopfer et al. 2015	David Anderson

2.2 BEHAVIORAL SETUPS

2.2.1 *Behavioral chamber*

The behavioral chamber, equipped with camera (Point Grey, sampling rate: 100 Hz, spatial resolution: 912 × 920 pixels) and 16 recording microphones (Knowles NR-23158, sampling rate: 10 kHz) was constructed as previously described (Arthur et al. 2013; Coen et al. 2014; Clemens et al. 2018) with one modification: instead of a mesh, we placed a thin, white paper directly on the microphones to pick up vibration signals. The behavioral chamber measured 44 mm in diameter and 1.9 mm in height, chamber and lid was made of transparent plastic. Chamber lids were coated with Sigmacote (Sigma-Aldrich) to prevent flies from walking on the ceiling, and kept under a fume hood to dry for at least 10 minutes. The chamber was illuminated with blue light-emitting diodes (LEDs) (470 nm) and for wild-type recordings also room light was switched on. Sound recording and video were synchronized by positioning a green LED that blinked with a fixed temporal pattern in the field-of-view of the camera and whose driving voltage was recorded alongside the song.

2.2.2 *Vibrometer*

The deflections of the substrate induced by vibrations were measured using a PSV-400 laser Doppler vibrometer (Polytec GmbH, kindly provided by Martin Göpfert). Fly pairs were placed into the same behavioral chamber as described above. The chamber floor was the same thin, white paper as used in all other recordings, taped to the bottom

of the chamber. The laser beam was directed through the lid perpendicular onto the paper surface 1-4 mm near the courting flies (Suppl. Figure 1.1).

2.2.3 *Zoom chamber*

We recorded courting OregonR flies in a zoom chamber which was only 11 mm wide and equipped with a higher spatial resolution camera (FLIR, sampling rate: 150 Hz, spatial resolution: 1200 × 1200 pixels) and only one microphone (Knowles NR-23158, sampling rate: 10 kHz), illuminated with white LEDs.

2.3 BEHAVIORAL ASSAYS

For all experiments, 3 to 7 day old naive males and virgin females were used. Wild-type experiments were performed with NM91 flies, except for recordings in the zoom chamber, for which we used OregonR. Flies were introduced gently into the chamber using an aspirator. To catch the morning activity peak, recordings were scheduled to start within 120 minutes of the behavioral incubator lights switching on. Free courtship recordings were performed for 30 minutes, in the zoom chamber for 10 minutes and in the vibrometer for maximal 2 minutes.

2.3.1 *Manipulations*

For experiments with abdomen cut males (Figure 1.2A-C), the abdomen was cut off with a sharp razor blade on ice prior to the experiment. The males recovered 5 minutes until two females were introduced to the chamber, to increase the chance that he would engage in courtship. Recordings with abdomen cut males were started once the male started courting one of the females.

In experiments using males with amputated wings (Figure 1.2D-F), the wings on both sides were amputated on ice the day before the experiment.

2.3.2 *Satiation assays*

For satiation assays (Figure 5) group-housed males were transferred individually into food containing vials together with 10-15 virgin NM91 females, and allowed to freely interact with them for 4-6 hours. The control group were groups of only males with the same genotype (pC2l > CsChrimson or P1a > CsChrimson). After this pre-exposure period, all flies were quickly anesthetized on ice to separate the male, who was gently transferred into an empty vial to rest for 15 minutes. Then he was gently introduced to the behavioral chamber to start optogenetic activation.

2.4 COURTSHIP SIGNAL ANALYSIS

2.4.1 *Signal annotation*

Courtship signals (pulse, sine and vibration) were manually annotated using the graphical user interface of deep audio segmenter (Steinfath et al. 2021). Signal annotation for optogenetic activation experiments with speed-controlled virgins or satiated males was performed blindly, without knowledge of the retinal supply or manipulation.

2.4.2 *Signal train definition*

We regarded all detected pulses as part of a pulse train if their inter-pulse interval (IPI) was within 80 ms from the next pulse and vibrations within an IPI of 400 ms as part of a train, which is about twice of their average IPIs.

2.4.3 *Signal fractions*

The signal fraction is the time fraction of all courtship frames (see Courtship index 2.5.2) in which signal trains were produced.

2.4.4 *Signal transitions*

To get transitions probabilities between signal trains, we scored how often a particular signal train type was followed by another out off all occurrences of the considered signal train type, regardless of the pause duration in between trains. Presented is the mean of such transition matrices for 11 NM91 wild-type couples.

2.4.5 *Signal probabilities*

For experiments with optogenetic neural activation or inactivation, the probability for a male to generate pulse, sine or vibrations at any point in time during a trial of a given stimulus block was computed as the fraction of trials containing pulse, sine or vibrations. We computed the mean across trials, pooling from the different males. For experiments with speed-controlled females (Figure 3) we only used courtship time points to compute the vibration probability.

2.4.6 *Waveform analysis*

Data obtained with the laser vibrometer were high-pass filtered (Butterworth, 60 Hz). Microphone recordings of the same signal on different microphones were regarded as one and the waveform was taken from the loudest channel. To compare vibrations measures with the vibrometer or microphones, we extracted 60 ms long waveforms from all time points annotated as vibration signal. To remove variability in the waveforms

arising from the position and distance of the singing male from the microphone, we normalized waveforms (also vibrometer waveforms) as described before (Clemens et al. 2018). Briefly: we divided the raw waveforms by their norm, centered them to their peak energy and flipped their sign such that the average of the 1 ms preceding the pulse center was positive. Vibrations recorded with a microphone had two distinct waveforms, resembling slow and fast pulse song (Clemens et al. 2018). We split them depending on the sign of the waveform 0.4 ms after the pulse center: if the waveform at this point was negative, we considered them as "fast" vibrations, else as "slow" vibrations. The same analysis on the vibrometer waveforms only yielded 9 "slow" out of 53 waveforms in total, which is why we pooled all waveforms from the vibrometer. Plotted in Figure 1.1C are only the central 12 ms of the waveforms. Frequencies were obtained by taking the center off mass from the Fourier transformed waveforms.

2.5 BEHAVIORAL DATA ANALYSIS

Pose tracking of flies (locations of head, thorax, leg and wing tips) were performed automatically using DeepPoseKit (Graving et al. 2019). All data for behavioral analysis were sub-sampled to 50 Hz.

To show traces of signal probabilities or velocities and wing angles for optogenetic experiments or onset/offset analysis (Figures 1.3,2.2), we pooled data across flies and computed the mean (for signal probabilities) or median (for velocities or wing angles) across stimulation trials or onsets and offsets. All traces shown for optogenetic experiments (Figures 3,4-7) are smoothed with a 1 s Gaussian window with a standard deviation of 0.1 s.

2.5.1 *Copulation detection*

Videos were automatically scored for copulation. When flies copulate, their distance drops for longer time periods below one fly length. We smoothed the distance trace with a running average of 10 s. Whenever the smoothed distance between two courting flies dropped below 2 mm and remained below for time windows of 30 – 180 s, expanding the time windows by 30 s consecutively, we would score this time point a successful copulation start. We did not directly check for a distance below threshold for a longer time window to cover cases where the copulation start was close to the end of the recording; in contrast only scoring for distances below threshold which last 30 s gave us false positives in exceptional cases of tracking errors or courtship close to the wall. We proofread all copulation starts and when detected wrongly, we corrected them manually. Data after copulation were excluded from analysis.

2.5.2 *Courtship index*

We considered all frames in which the male was within a distance of 8 mm (6 mm for GLM analysis) relative to the female and his relative angle to her within 60° as courtship

frames. The courtship index is the fraction of these courtship frames from all recorded frames until copulation started or the recording ended.

2.5.3 *Wing extension*

To compute wing angles, we extracted the positions of wing tips and the center line of the head and thorax in each frame. We used DeepPoseKit (Graving et al. 2019) to automatically annotate wings and the center line of the head and thorax. Wing angles were normalized to fall in the range [-180°, 180°] with angles > 0° denoting wing positions away from the center line. When at least one wing angle was between 25 - 100°, we scored it as a wing extension.

2.5.4 *Stationarity*

To find the frames in which flies were stationary, we smoothed velocity magnitude traces with a running average of 2 s. Due to tracking noise, our velocity data never reach zero. Next, we obtained the frames in which the smoothed velocity dropped below 0.48 mm/s. The smoothing blurred the actual time points when the flies stopped or initiated walking again. To account for this, we traced stationarity onsets of each immobility phase back to the time point where the raw velocity initially dropped below 0.95 mm/s and expanded the immobility phases accordingly. Similarly, we expanded the immobility phase to the time point where the raw velocity exceeded 0.95 mm/s.

2.6 OPTOGENETICS

Flies were kept for at least 3 days prior to the experiment on fly food supplied with retinal (1 ml all-trans retinal (Sigma-Aldrich) solution (100 mM in 95% ethanol) per 100 ml food). To shield flies and retinal from light, the vials were wrapped in aluminium foil. To prevent the LED light stimulation from interfering with the video recording and tracking, we used a short-pass filter (Techspec, blocking wavelengths: 512 - 715 nm) on the camera's objective. Control flies were either parental controls (only Figure 4) or had the same genotype as experimental flies and were kept on regular food without additional retinal.

2.6.1 *Optogenetic inactivation*

GtACR1 (Mauss, Busch, and Borst 2017) was inactivated using a green LED at 525 nm wavelength. For vGlut inactivation (Figure 3A,C) we used a green light intensity of 9 $\mu W/mm^2$ (driving voltage 1.32 V). Each experiment started with a pre-stimulation time of 40 s with green LEDs switched off, followed by 40 trials of optogenetic inactivation (however, we excluded the last trial for all data shown here). Each trial started with 5 s optogenetic stimulation, followed by 25 s pause with green LEDs switched off until the next optoge-

netic inactivation started, every 10^{th} trial, the pause until the next inactivation was 65 s.

2.6.2 *Optogenetic activation*

CsChrimson (Klapoetke et al. 2014) was activated using a red LED at 625 nm.

For DNp28 activation (Figure 3B,D) we used a red light intensity of 57 $\mu W/mm^2$ (driving voltage 1.5 V). Each experiment started with a pre-stimulation time of 15 s with red LEDs being off, followed by 31 trials of optogenetic activation (however, we excluded the last trial for all data shown here). Each experimental trial started with 5 s optogenetic stimulation, followed by 25 s pause with red LEDs being off until the next optogenetic activation started.

For pC2l and P1a activation (Figures 4-7) we used a red light intensity of 27 $\mu W/mm^2$ (pulsed driving voltage 1.32 V). Each experiment started with a pre-stimulation time of 40 s with red LEDs switched off, followed by 7 trials of optogenetic activation (however, we excluded the last trial for all data shown here). Each experimental trial started with 5 s optogenetic stimulation, followed by 120 s pause with red LEDs switched off until the next optogenetic activation started.

2.7 GENERALIZED LINEAR MODEL ANALYSIS

2.7.1 *Behavioral cues*

We used multinomial GLMs (also known as multinomial logistic regression) to predict which of three signal types (no signal, song and vibration) a male will produce at an arbitrary moment in time. For this, data from tracked fly trajectories (Graving et al. 2019) of 14 NM91 couples were transformed into a set of 19 feedback cues (using xarray-behave, Table 2): male or female rotational speed, rotational acceleration, velocity magnitude, lateral velocity, forward velocity, acceleration magnitude, forward acceleration, lateral acceleration as well as the relative distance between flies and the relative angle and relative orientation of the male to the female. We only used courtship time points (distance below 6 mm between flies and a relative angle of < 60° between male and female) and excluded time points after copulation. To eliminate tracking errors from our data set, we excluded data points where the distance between male and female dropped below 1 mm as well as data points where DeepPoseKit (Graving et al. 2019) predicted a fly head or thorax with with less than 50% confidence. Cues were z-scored and pooled across flies so that each GLM could be fitted to the data from an entire population. For each cue, we extracted numerous time windows of 1 s before the current signal event; for this each window was shifted in time by one frame relative to the previous window (time-delay embedding from GLM utilities, Table 2). Each window represents the history of 1 s for each given cue prior to a signal event, like song or vibrations, at an arbitrary moment in time. Subsequently each of these time-delay embedded cue windows was projected to a basis of four raised cosines by forming their dot product, to reduce dimensionality (raised cosine from GLM utilities, Table 2, based on Weber and Pillow 2017).

Finally, data were balanced, i.e. randomly sub-sampled to contain an equal number of vibration, song and no signal events. This yielded 73562 time points per signal type that were considered as inputs to the models for male communication behavior.

2.7.2 *GLM implementation*

Data points of behavioral cues were split into 90% training data and 10% test data. We fitted models over 10 iterations, with randomly sub-sampling and randomly splitting into training and test data each cycle. To avoid overfitting, all multinomial GLMs were fitted with a l2 regularization penalty (ridge regression), a 10-fold cross validator and a maximum of 500 iterations (LogisticRegressionCV from scikit learn, (Pedregosa et al. 2011)).

Once a model was trained, we assessed the model's performance by predicting signal events on test data. With this, we obtained the confusion matrix of a model, a table that maps the actual outcome from the test data to the predicted outcome from the trained model. The diagonal of the presented confusion matrix depicts true positive predictions of the model (false negatives are (100% - true positives)) whereas the off-diagonal elements show false positives. Furthermore, we scored the model's classification accuracy which is the proportion of correct predictions over total predictions. To yield the cue importance of the full model, we shuffled one cue at a time in the test data set and quantified the reduction in model accuracy.

2.7.3 *Variance analysis*

To quantify upper and lower bounds on the explanatory power of each cue, we computed for each cue the unique contribution and overall explained variance (Musall et al. 2019).

To obtain a cue's unique contribution, that is its contribution to the predictive accuracy of the full model, we fitted reduced models. In these models we shuffled one cue at a time in the training data but kept all other cues the same. The reduction in accuracy compared to the full model gave us the unique contribution of each cue.

To obtain the explained variance of each cue, we trained reduced models where all cues apart from the specified one were shuffled. We then tested these single-cue models on test data and scored their accuracy as explained variance of the specified cue.

For the one-cue models, linear filter shapes were extracted by back-projecting the raised cosine basis to the model's coefficients. Summing the resulting time-domain filter along the time axis gave us filter sums. We obtained true positive diagonals of the single-cue model's confusion matrices.

2.8 STATISTICAL ANALYSES

We obtained the mean of signal probabilities and the median of velocity magnitudes or wing angles computed across trials for each tested fly and the median of vibration

amplitudes for each tested fly. We tested data between flies for significance with the tests indicated in Figure captions. For waveform comparison (Figure 1.1) we compared waveforms pooled from a single fly couple for each set-up. To check for normality we performed Shapiro-Wilk tests.

All box plots present the quartiles of the data set; the inner line is the median of samples; whiskers represent minimum and maximum values, except for points that are determined to be "outliers". Outliers are determined with a method which is a function of the inter-quartile range (seaborn, Table 2).

Table 2: Software and Algorithms.

RESOURCE	IDENTIFIER
DeepPoseKit	`https://github.com/jgraving/DeepPoseKit` (Graving et al. 2019)
DeepAudioSegmenter	`https://github.com/janclemenslab/das` (Steinfath et al. 2021)
GLM utilities	`https://github.com/janclemenslab/glm_utils`
Inkscape 0.92	`https://inkscape.org`
Python 3.7	`https://python.org`
scikit learn	LogisticRegressionCV from `https://scikit-learn.org` (Pedregosa et al. 2011)
seaborn	plots (e.g. boxplot) from `https://seaborn.pydata.org`
xarray-behave	`https://github.com/janclemenslab/xarray-behave`

3

RESULTS

The NM91 wild-type experiments used for analysis in Figure 1, 1.3, 2, 2.1, 2.2 and 2.3 were performed and annotated by Afshin Khalili (postdoctoral research fellow in the Clemens lab), a portion was annotated by Melanie Stenger (former master student under my supervision, now graduate student in the Clemens lab). Afshin Khalili started off with the multinomial GLM (full model) analyses presented in this thesis which I revised. I introduced the reduced models to our GLM analyses. He initially found that P1a and pC2l drive vibrations and had preliminary results on state and cue modulation of P1a, however his results are not presented in this thesis. I reproduced these findings with slightly altered experimental parameters and extended them by investigating state modulation on solitary males as well as state and cue modulation of pC2l. Melanie Stenger performed the OregonR wild-type experiments in the zoom chamber (Figure 1.1). The experiments for DNp28 (Figure 3) were performed and annotated by Jannis Hainke and Tina Zahrie (rotation students under my supervision). Annotation of experiments in Figures 4, 6 and 7 were partially completed in collaboration with Melanie Stenger, Maximilian Ferle (student assistant) and Kimia Alizadeh (lab technician). I extensively proofread all annotations.

3.1 COURTING MALES PRODUCE DISTINCT SIGNAL TYPES: SONG AND VIBRATIONS

3.1.1 *Recording song and vibrations in a behavioral chamber*

To assess the coordination of song and vibrations, we needed a system for recording both signals at the same time in courting males. So far, song and vibrations have been recorded separately. Courtship song and behavior are usually recorded in a behavioral chamber lined with a mesh, equipped with a camera and microphones. Fly poses are tracked and courtship song is annotated automatically from video and audio data (Arthur et al. 2013; Coen et al. 2014). Fly behavior like male abdomen quivering, wing fluttering and female immobility associated with vibrations has been quantified by manual, visual video inspections, yielding a lower time resolution than for song studies. Vibration signal shape was picked up with laser vibrometers (Fabre et al. 2012; Mazzoni, Anfora, and Virant-Doberlet 2013; Hernández and Fabre 2016). To record both signals, we modified the behavioral set-up commonly used in fly song studies. The flies interacted in a chamber with a camera on top and a thin paper on the bottom. The paper was placed directly on microphones to enable the recording of substrate-borne vibrations (Figure 1A). The modified set-up provided us with high time resolution data of courting fly interactions alongside reliable recordings of male song and vibration signals (Figure 1B-C).

To validate our rig, we manually annotated pulse song, sine song and vibration from courting wild-type males in the audio recordings. First, we confirmed that we detect

song as reliably as in a chamber commonly used to record song (Arthur et al. 2013; Coen et al. 2014). The paper substrate is less permeable for air-borne signals than a mesh, this slightly dampened song amplitude. Additionally the paper transmits various substrate deflections, accordingly also walking noise and other movements are recorded. Even though our song data were slightly more noisy due to the paper substrate, males sang pulse and sine as frequently as reported with other chambers (Figure 1E, our chamber: 8% pulse, 6% sine of courtship time; Coen et al. 2014: 20% song of courtship time). Also train lengths of pulse and sine (0.3 and 0.4 s) correspond to observations in other set ups (Figure 1G, Arthur et al. 2013; Coen et al. 2014).

Next, we confirmed that the vibrations we pick up with microphones are comparable to vibrations recorded with a laser vibrometer (Suppl. Figure 1.1A). For vibrations recorded with microphones we found two distinct waveforms, resembling fast and slow pulse song (Clemens et al. 2018), but the same analysis yielded only 9 slow out of 53 total waveforms which is why we pooled both types for the vibrometer. Additional future vibrometer recordings will reveal if the distinct waveforms are reliably detectable by measuring surface deflections. The waveforms of single fast vibration pulses and the intervals between one vibration pulse and the next one (IPI) are similar when recording courting flies in a vibrometer or our set-up (Figure 1F and Suppl. Figure 1.1B,C). Similarly, the carrier frequency of fast vibrations recorded with the microphones was comparable to the frequency picked up with the vibrometer, only the carrier frequency of the slow waveforms recorded with microphones was slower by about 100 Hz (Suppl. Figure 1.1B). This is in line with the broad frequency spectrum of vibrations measured with a vibrometer on different fruits or membrane (McKelvey et al. 2021). In previous studies vibration generation was quantified by male abdomen movements ("quivering") which coincide with vibrations (Fabre et al. 2012). Using a behavioral chamber with a high resolution camera, we confirmed that the vibrations we pick up with our microphones are similarly associated with abdominal quivering. Matching the abdominal quivering from the videos with the vibration signals annotated in the audio recordings, we find an overlap of both read outs (Suppl. Figure 1.1D-E).

3.1.2 *Song and vibrations are produced with different body parts*

The male sings the courtship song using one wing at a time. However, when he produces vibration signals, his wings are mostly closed (Figure 1D) and wing cut males still produce vibrations (Suppl. Figure 1.2D-F, Fabre et al. 2012). We concluded that vibrations are generated by the male with another body part than his wings. Although vibrations have been described previously to sometimes occur simultaneously with wing extension (Fabre et al. 2012), we find that song production and vibrations hardly overlap. Vibrating males have open wings 19% of the vibration time but males rarely sing pulse or sine when vibrating (Suppl. Figure 1.3A). This suggests that even though the male is physically able to sing and vibrate at the same time (and we can pick it up in our set-up), the two signals tend to be mutually exclusive.

Vibrations coincide with quivering abdomen movements (Fabre et al. 2012). When cutting the male abdomen we still observe vibration production of the courting male

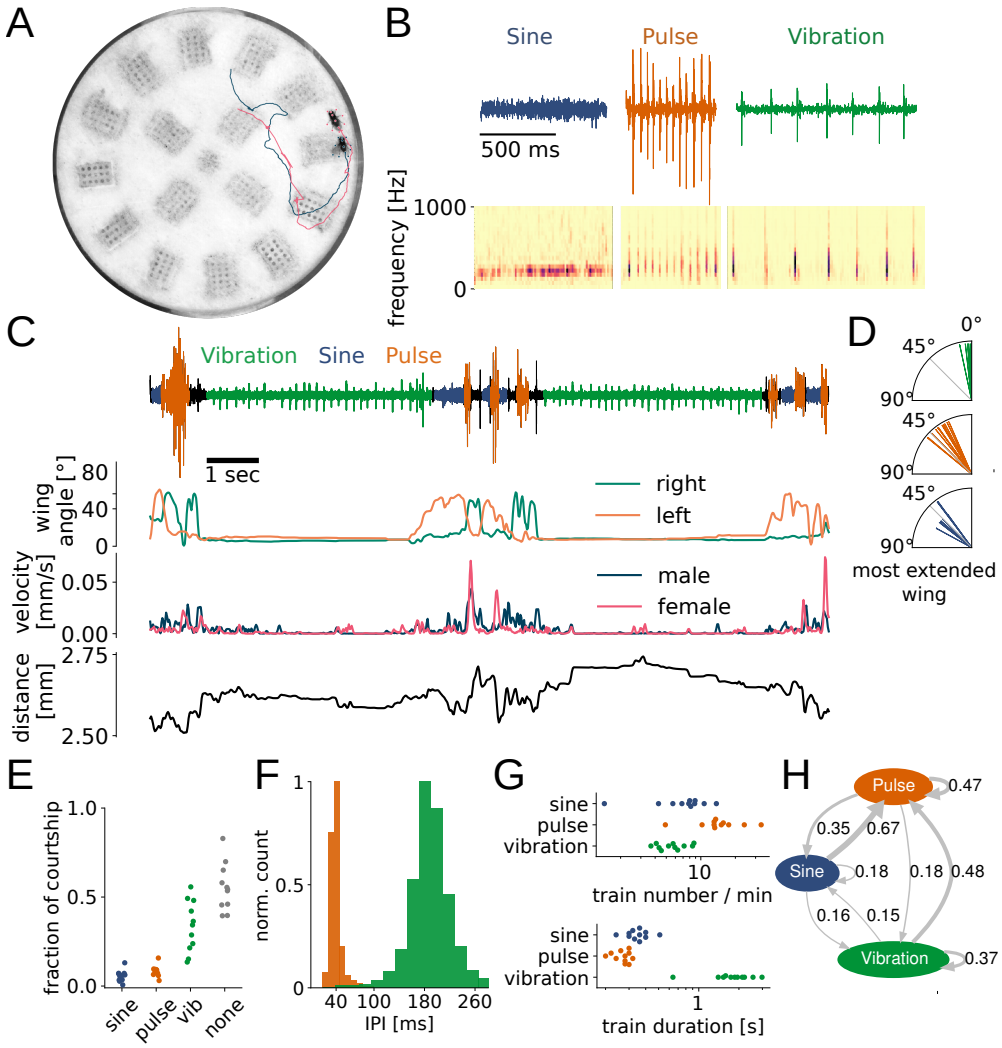

Figure 1: **Courting males produce distinct signal types: song and vibrations.**
A Behavioral chamber with courting fly couple. Tracked poses and walking trajectories are shown for male (blue) and female (pink). **B** Waveforms (top) and spectrograms (bottom) for examples of sine (left), pulse (middle), and vibration (right). The spectrogram shows the signal's frequency content over time. **C** Example audio trace with vibration (green), sine (blue) and pulse (orange) signals and corresponding behavioral cues extracted from pose tracking: left and right wing angle of the male, velocity magnitude of male and female and distance between them. **D** Median angle of the most extended wing for all courtship signals: vibration (12° ± 5), pulse (48° ± 9) and sine (58° ± 8) (from top to bottom), n = 11 flies. **E** Signal type fraction of courtship time (mean ± std): sine (6% ± 3), pulse (8% ± 3), vibration (24% ± 10) and no signal (62% ± 11), n = 11 flies. **F** Inter-pulse interval for pulse song (37.4 ms ± 9.4, orange) and vibration (180.1 ms ± 38.1, green) (10000 pulse samples and 13000 vibration samples, IPIs below 70 ms and 360 ms are excluded, respectively). **G** Number of signal trains per courtship minute (top) for sine (7.7 ± 3), pulse (15.8 ± 7) and vibration (5.8 ± 2). Duration of signal trains (median ± std): sine (0.35 s ± 0.07), pulse (0.27 s ± 0.04) and vibration (1.87 s ± 0.59) (log scale, n = 11 flies). **H** Transition probabilities between signal trains, n = 11 flies.

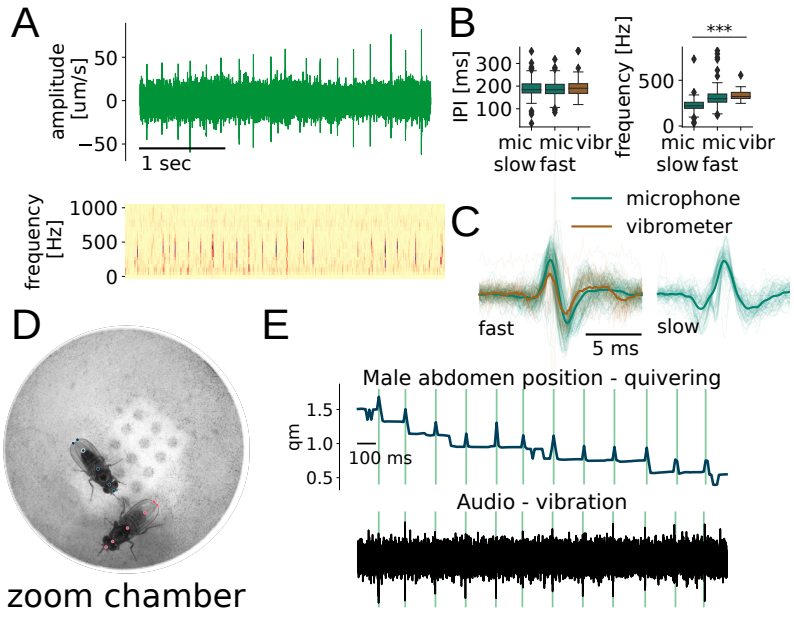

Suppl. Figure 1.1: **Vibrations deflect the substrate surface and coincide with abdomen movements.**

A Vibration measured with laser vibrometer (top) and the corresponding spectrogram (bottom) with the signal's frequency content over time. **B** Inter-pulse interval for vibration train are similar when measured with microphones (184 ms ± 45 (slow), 184 ms ± 39 (fast)) or a laser vibrometer (190 ms ± 46 ms), p = 0.33 (slow), p = 0.13 (fast), t-test. IPIs above 360 ms are excluded. Frequency of slow vibration waveforms (right) recorded with microphones (221 Hz ± 81) but not fast vibration waveforms (298 Hz ± 108) are different than waveforms recorded with vibrometer (323 Hz ± 53), p = 1 x 10^{-16} (slow), p = 0.15 (fast), t-test. **C** Average (thick line) and single vibration waveforms (12 ms duration). Here (B-C), we show data of vibrations measured with microphones of our behavioral chamber (n = 147 fast, 97 slow waveforms, n = 1 fly couple) or in a laser vibrometer (n = 53 waveforms, n = 1 fly couple). **D** Zoom chamber with courting fly couple on top of the single microphone. Poses of tracking are indicated. **E** Male abdomen position (top) is tracked with high spacial resolution in the zoom chamber. Abdomen movements correlate with vibration signals in the audio trace (below).

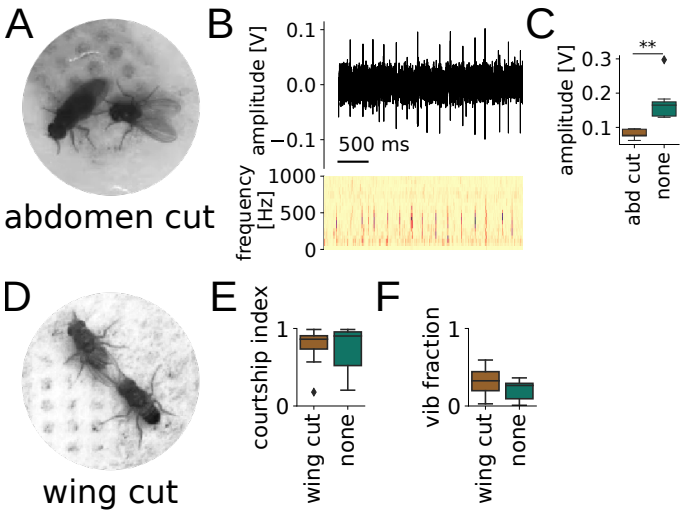

Suppl. Figure 1.2: **Abdomen cut and wing cut males still vibrate.**
A An abdomen-cut male courts a female. **B** Raw microphone trace of vibration signal elicited by an abdomen-cut male (top) and spectrum (bottom). **C** Abdomen-cut males vibrate at lower amplitude (0.08 V $\pm$ 0.01) than intact males (0.17 V $\pm$ 0.05), p = 0.007, t-test, n = 5 abdomen-cut, n = 7 intact males. **D** A wing cut male courts a female. **E** Wing cut males court as much as intact males, courtship index 0.86 $\pm$ 0.25 and 0.90 $\pm$ 0.27, p = 0.78, t-test, respectively. **F** Wing cut males vibrate as much as intact males, fraction of vibration in courtship for wing cut and intact males: 0.32 $\pm$ 0.16 and 0.26 $\pm$ 0.12, respectively, p = 0.14, t-test, n = 8 wing-cut, n = 9 intact males.

(Suppl. Figure 1.2A-B, Zhang, Rogulja, and Crickmore 2016), although with a lower amplitude (Suppl. Figure 1.2C), this suggests that the abdomen movement is not causal for the vibration production. A lower body weight of the abdomen cut male could be the reason for a lower vibration signal amplitude. Males without wings or without abdomen still vibrate, which body part or motor neurons generate them, remains to be found.

3.1.3 *Vibration signals span longer time scales than song*

We explored the temporal dynamics of vibration signals in comparison to song. Wild-type flies courted vigorously in our set up (courtship index: 0.6 $\pm$ 0.2). We found that males spend much more time vibrating then singing (Figure 1E). Within a train, the inter-pulse interval of vibrations is much longer than that of pulse song (Figure 1F). Vibration trains are much longer than pulse or sine trains but occur less often (Figure 1G). Thus, vibrations span longer time scales and males spend much more time producing vibrations than song.

3.1.4 *Males dynamically switch between signal types*

In courtship, the male dynamically switches between sine, pulse and vibrations. All courtship signals are most often followed by a pulse train and males switch more often between the two song types than between song and vibration (Figure 1H).

Males switch between sine and pulse song modes without interleaving pauses (6 ms). By contrast, song and vibration are typically separated by a 1 s pause (Suppl. Figure

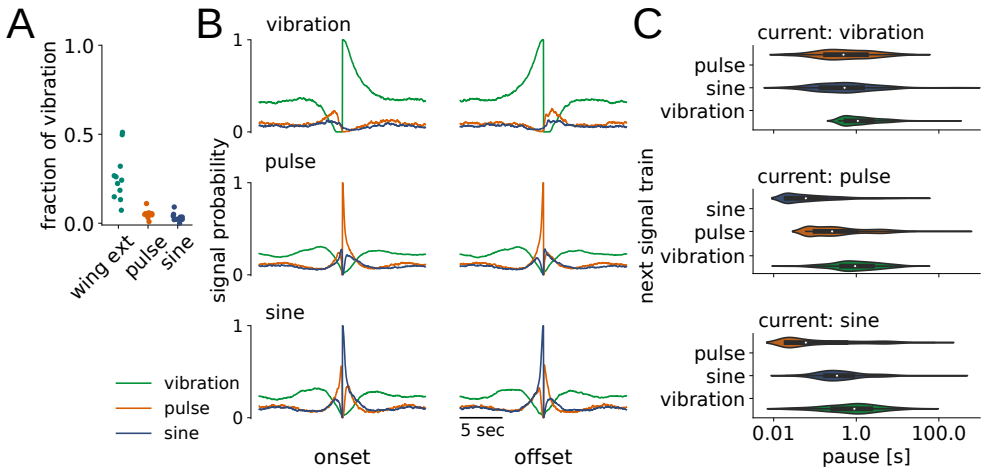

Suppl. Figure 1.3: **Little overlap and slow transitions between song and vibration.** **A** Vibrating males sometimes extend wings when vibrating (19.4% ± 14.0) but rarely sing (0.2% ± 0.5 pulse or 1.2% ± 1.7 sine song during vibration), n = 11 flies. **B** Probabilities of signal types centered to the onset (left) and offset (right) of each signal type: vibration (green, n = 906 trains), pulse (orange, n = 2783 trains) and sine (blue, n = 1338 trains) (from top to bottom). Note that pulse and sine transitions are closely aligned in time. **C** Pauses between signal trains (log scale), see Table 3.

Table 3: Pauses between signal trains.

CURRENT	NEXT SIGNAL TRAIN	PAUSE [S]	± STD
pulse	pulse	0.26	10.28
pulse	sine	0.06	1.84
pulse	vibration	0.94	3.06
sine	pulse	0.06	4.04
sine	sine	0.34	12.08
sine	vibration	0.90	3.89
vibration	pulse	0.49	2.95
vibration	sine	0.52	26.17
vibration	vibration	1.09	10.77

1.3B-C, Table 3). Immediate transitions or even overlaps between song and vibration are rare. Instead of randomly alternating between the signal types, the male produces some combinations more likely than others. We hypothesized that the male selects each signal in a distinct behavioral context.

Song and vibrations are two different communication modalities: song is generated by wing movement and transmitted through the air to the female (Yamamoto and Koganezawa 2013). In contrast, vibrations are transmitted through the substrate and were shown to be picked up by females with their leg mechanosensory neurons (McKelvey et al. 2021). The male has the choice to produce either signal: song or vibrations. In which situation will he choose one modality over the other?

3.2 SIGNAL CHOICE IS MODULATED BY DISTANCE AND LOCOMOTION

From courtship song, we know that males sing and also switch between song types based on sensory feedback cues from the female (Coen et al. 2014; Clemens et al. 2018; Calhoun, Pillow, and Murthy 2019). To find the cues which inform the male to choose

between song and vibration, we employed multinomial generalized linear models (GLMs). These models allow us to estimate which cues inform male signal choice and how a given cue is integrated over time to best predict signal choice, in an unbiased fashion. The model's input are feedback cues such as distance and orientation between male and female as well as their movements. The cues are passed through a linear filtering stage, with a separate set of filters for each signal type (song, vibration, no signal). Then the models pass the filters through a nonlinearity and transforms them to probabilities of each signal type output (Figure 2A).

First, we trained a multinomial GLM to predict song, vibrations or neither signal from all 19 feedback cues. This full model predicts vibration correctly by 83%, song by 68% and no signal by 46% (Figure 2B), yielding an overall accuracy of 65%. We predicted vibration with a surprisingly high accuracy, suggesting that vibrations are associated with a stereotypical behavioral context.

Feedback cues define a behavioral context. If a particular context is associated with a signal preference of the male, a defined set of cues will be important to predict either signal output. Some cues could be necessary for our model to predict a male's signal choice and others even sufficient. For example in courtship, the male closely tracks the females and follows her as she moves around the chamber. Accordingly, male and female movement are closely correlated and some redundant cues could compensate for one another in the full model. We decided to investigate which cues are necessary by finding how much each cue contributes to the predictive accuracy of the full model. For this we fitted reduced models in which we shuffled one cue at a time in the training data but kept all other cues the same. The resulting loss of accuracy compared to the full model measures the amount of non-redundant information that each cue contributes to the model, shortly each cue's unique contribution (Musall et al. 2019). The unique contribution of most cues ranged around 0 (Figure 2C, left), demonstrating that they could compensate each other's contribution to the model's performance or were not necessary for the model in the first place. Only distance, female velocity magnitude and male lateral velocity significantly reduced the model's performance when shuffled, indicating that they're required for predicting signal choice (Figure 2C, left).

3.2.1 *Males sing when close to the female.*

Above we analysed the contribution of individual features to the overall signal prediction of our model to find which cues are necessary for an accurate prediction. But it is still unclear if the male relies on different cues to decide between singing and vibrating. To disentangle which cue is sufficient for predicting vibrations and which for song, we fitted single-cue models. For this all cues but one were shuffled at a time and we asked how well each model could predict the different signal types (Musall et al. 2019). The prediction accuracy of these reduced models give us the explained variance of each feature, a measure of their explanatory power in predicting signal choice. A high explained variance of a cue indicates that a cue is sufficient for an accurate signal prediction.

First, we focus on distance, since it had the highest unique contribution to the full model. A model relying solely on distance only explained 47% (Figure 2C, right). The com-

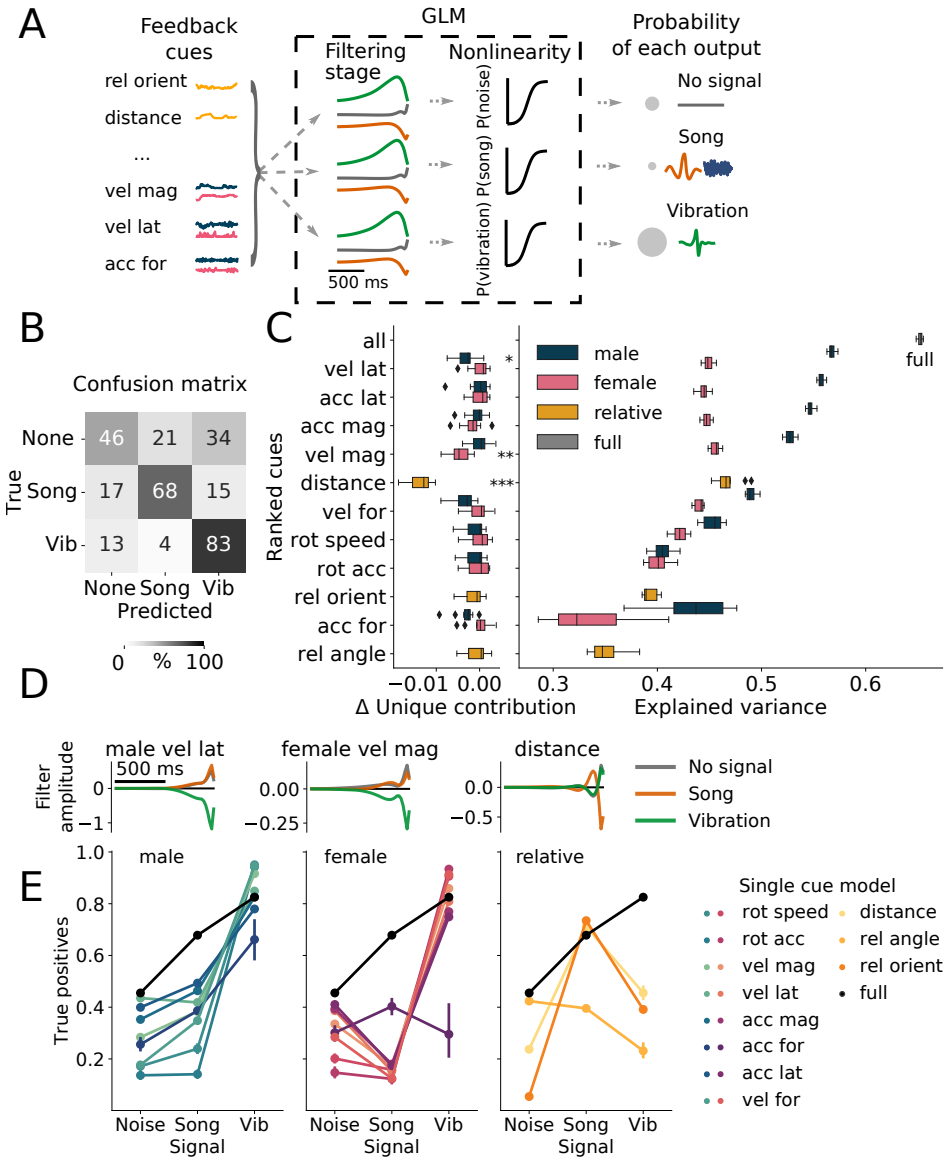

Figure 2: **A reduction in speed predicts vibrations and a low distance predicts song.** **A** Schematic illustrating the multinomial GLM (modified from Calhoun, Pillow, and Murthy 2019), which takes feedback cues as input and passes these cues through a linear filtering stage. There is a separate set of linear filters for each possible signal. These filters are passed through a nonlinearity step, and the relative probability of observing each output (no signal, song, vibration) gives the overall likelihood of song production. **B** Confusion matrix for the full model predicting song, vibration or no signal on the test data set. Shading and text labels indicate the percentage (see color bar). **C** Δ Unique contribution and explained variance for single behavioral cues of male (blue), female (pink), relative (yellow) or all cues in the full model (grey). Each model was run for 10 different random states. In models with shuffled male vel lat, female vel mag or distance, the prediction accuracy significantly drops ($p = 0.0016$, $p = 0.0002$, $p = 1.5 \times 10^{-10}$, t-test, significance level corrected to $p = 0.0025$ by Bonferroni) compared to the full model. The difference between the full models's accuracy and the shuffled models yields the unique contribution. **D** GLM filters for male velocity lateral (top), female velocity magnitude (middle) and distance (bottom) for all three signal types. A reduction in male and female velocity is predictive for vibration (green) and a low distance is predictive for song production (orange). **E** True positive prediction probability (diagonal of confusion matrix) for single feature GLMs. Male cues predict vibrations very well and song moderately. Female cues only predict vibrations well and relative distance predicts song well. Presented in black are the true positive prediction probabilies of the full model for comparison.

bination of distance's highest unique contribution to performance with its intermediate explanatory power indicated that the model uses distance for predicting only some signal. Asking which signal distance predicts best, we found that a distance-based model predicts vibrations poorer (true positives 46%) but song equally well as the full model (71% true positives). We noted that the distance model predicts song better than any other single-cue model (Figure 2E, right). This combination of high unique contribution and accurate song prediction makes distance the most predictive cue for song choice.

The performance analyses above indicate that distance matters for a song prediction, but does not tell how distance influences song choice. To find how a given sensory cue is integrated over time to best predict future signal choice, we inspected the GLMs' linear filters (also called coefficients). Filters describe how the model linearly transforms the history of a cue to predict a signal event. The filter to predict song of the distance-only-model is negative right before the predicted event (Figure 2D, right), indicating that low distances are associated with song choice. We further inspected the tuning curves of signal type output based on distance. Tuning curves depict the output probability of a given signal type as a function of the cue of interest. The highest probability for a male to sing sine or pulse song is at low distances, below 3 mm (Suppl. Figure 2.3A, right), confirming that the male prefers to sing when close to the female. The male's position relative to the female is strikingly more broad when he is vibrating, compared to singing (Suppl. Figure 2.3E), making distance a very unreliable predictor for vibrations. Distance has been shown before to be the most informative cue for the male to switch between sine and pulse song (Coen et al. 2014) as well as between fast and slow pulse song (Clemens et al. 2018). Apparently, distance not only informs the male's switch between the different song modes but is also the predictive cue for an overall song output preference. This is also nicely in line with former studies which showed that the male generally sings courtship song when close to the female and that, next to distance, it is different behavioral states, associated with his movements, which strongly bias him in his song mode choice (Calhoun, Pillow, and Murthy 2019).

3.2.2 *Males vibrate when male and female are immobile.*

Next we focused on the speed-related cues. Most speed-related cues could compensate each other's contribution to the model's performance (Figure 2C, left), indicating that they are not necessary for a good model prediction. But some models based on a single speed cue reached high explained variances, indicating that these speed cues are sufficient for a good signal prediction. Four models relying on a male movement cue alone could explain above 53% of variance each. In contrast, female movement cues alone never exceeded 46% (Figure 2C, right). This gap in explained variance between male and female cues is explained by the observation that single male movement cues, which reached explained variances over 50%, predict not only most vibrations (83 - 92% true positives) but also some song correctly (38 - 49% true positives, Figure 2E, left). Whereas all female movement cues only predict vibrations well (75 - 93% true positives, excluding female forward acceleration) but song poorly (12 - 18% true positives, excluding female forward acceleration, Figure 2E middle). In short: both female and male movement cues

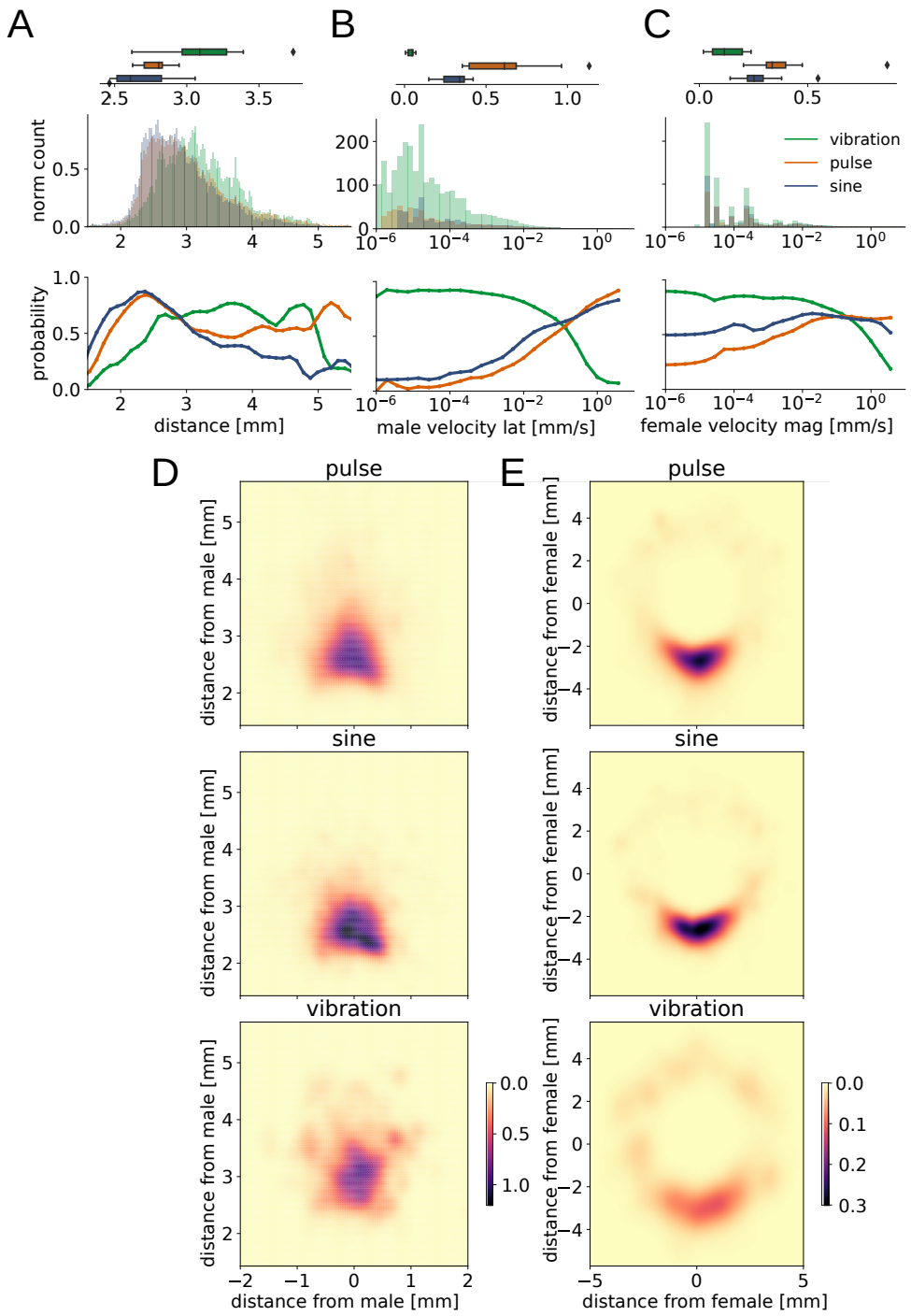

Suppl. Figure 2.1: **Males sing when close to females and when moving.**
A Distance between flies (top), distribution of distance between flies (middle) and tuning curve of distance between flies (bottom) for vibration (3.1 mm ± 0.3), pulse (2.8 mm ± 0.1) and sine (2.6 mm ± 0.2). The males sing when close to the female and vibrate when further away. **B-C** Same as in (**A**) for male lateral velocity when producing vibration (0.05 mm/s ± 0.02), pulse (0.61 mm/s ± 0.26) and sine (0.34 mm/s ± 0.09) (**B**) and female velocity magnitude when producing vibration (0.12 mm/s ± 0.08), pulse (0.34 mm/s ± 0.18) and sine (0.25 mm/s ± 0.11) (**C**). Low velocities of male and female are associated with vibrations, slow movement with sine and fast movement of the male with pulse. Quantified are median ± std for medians of n = 11 flies. Data for histograms and tuning curves are 49476 - 182438 data points pooled from n = 11 flies. **D** Position of the female relative to the male for pulse (top), sine (middle) and vibration (bottom). **E** Position of the male relative to the female for pulse (top), sine (middle) and vibration (bottom). Data for density plots are 27612 - 78796 data points pooled from n = 11 flies.

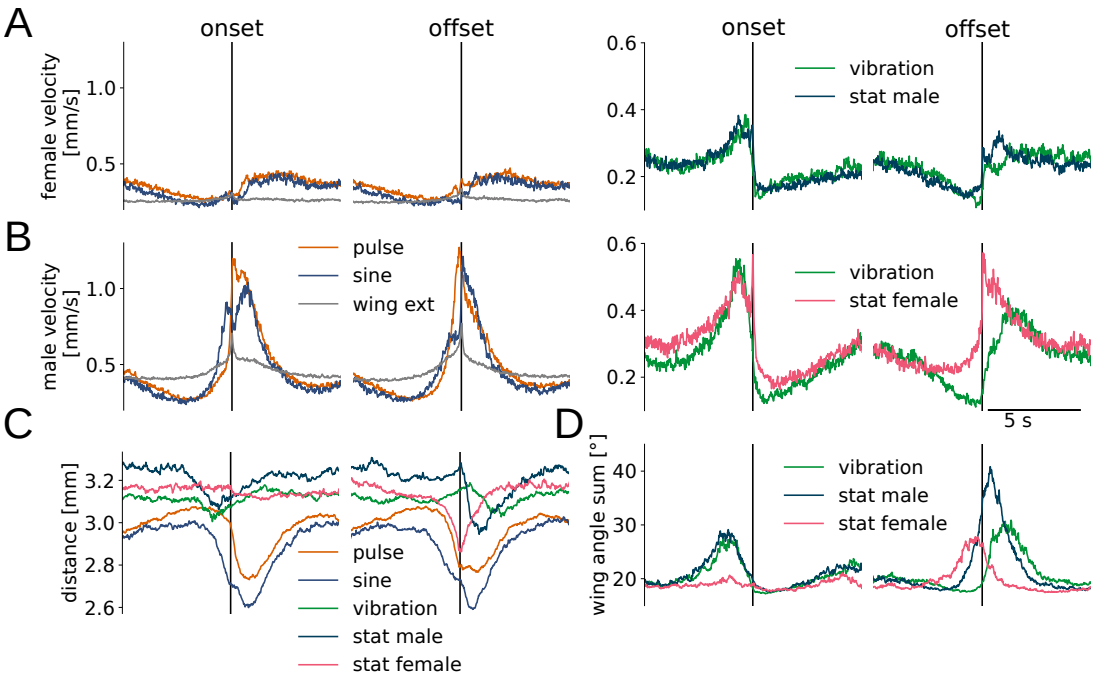

Suppl. Figure 2.2: **Changes in behavioral cues often align with signal onsets and offsets.** **A** Female velocity magnitude around the onset and offset of pulse, sine or wing extension (left) and around the onset and offset of vibration and male stationarity (right). **B** Same as in **A** but for male velocity magnitude. **C** Distance between flies around onset and offset of pulse, sine, vibration, male and female stationarity. **D** Wing angle sum of the male around onset and offset of vibration, male and female stationarity. Data represent medians for 903 - 11333 onsets/offsets pooled from n = 11 flies.

predict vibration very well, but only male movement additionally contains information for song.

To find the time course of movements that were predictive of vibration decisions, we inspected the filter shapes of male lateral velocity and female velocity magnitude which explained most of the variance from male and female cues and had a significant unique contribution (Figure 2C). The filters to predict vibrations are low pass filters and hereby reveal that decreases in speed predict vibrations. The filters to predict song are mainly high pass filters, showing that increases in speed predict song but also no signal (Figure 2D, left and middle). This trend holds for all speed-related filters of the single-cue models for which we got exclusively negative speed-filter sums predicting vibrations and positive sums for song (Suppl. Figure 2.3B). The tuning curve for male and female velocity show that vibrations were in fact associated with male and female immobility (median velocities of 0.1 mm/s for both males and females, Suppl. Figure 2.3A-B), which is in line with former findings of a strong link between female immobility and male vibrations (Fabre et al. 2012).

We concluded that male or female slowing or immobility predict vibration accurately whereas low distances and increases in male movement predict song choice.

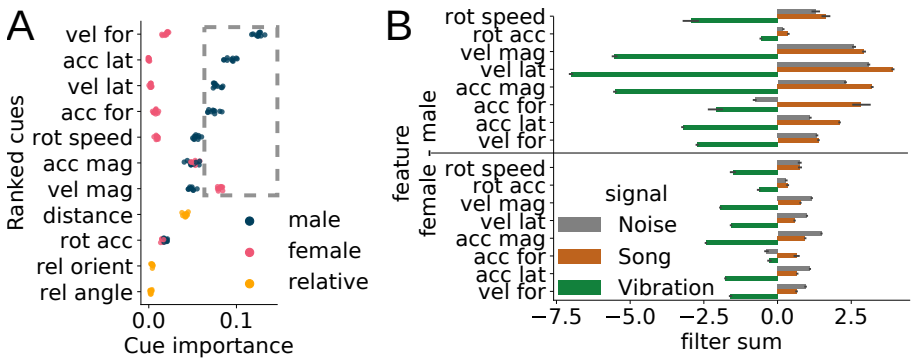

Suppl. Figure 2.3: **Vibrations are predicted by a decrease in speed.**
A Cue importance of each behavioral cue in full model. For this, only the indicated cue gets shuffled in the test data and the reduction in accuracy yields the cue importance. **B** Sum of linear filters for single cue models. Only speed-related cues for male (top) and female (bottom) are shown to illustrate that vibrations are predicted by negative speed cues and song by positive.

3.2.3 *Female immobility triggers male vibrations.*

Statistical modeling is a useful tool to investigate data in an unsupervised fashion. GLMs pick up correlations in the data to predict future behavior but cues used by the models to make prediction are not necessarily causal. Our models clearly point to the idea that female immobility is the cue directing the male's vibration behavior. To test the models causally, we manipulated female speed during courtship. We predicted that female stopping promotes vibrations and female acceleration suppresses vibration production of males.

First, we caused female immobility by optogenetically inhibiting all her motor neurons (Mauss, Busch, and Borst 2017) and let the male court this female freely. Stopping the female also induced male stopping and increased vibrations by 30%. As soon as the females could walk again, the males also increase in speed and vibration production dropped to baseline (Figure 3A,C). Second, we induced forward walking in females by activating the descending neuron DNp28 (Bidaye et al. 2020). DNp28 activation made the females speed up to 10 mm/s and also triggered increased male speed. Female and male forward walking almost completely abolished vibrations (Figure 3B,D). We noticed that the baseline of fly velocities were similar in both groups (with vGlut or DNp28 females) but that the vibration probabilities outside the optogenetic stimulation were different. Future analysis will reveal if females of both groups differ in stopping behavior which could explain such an effect.

Previous studies argue that male vibrations induce female immobility (Fabre et al. 2012). Our findings support a new perspective in which female immobility is the sufficient cue to induce vibration production in a courting male and female walking initiation in contrast makes him stop vibrating. As male and female speed are closely correlated in courtship, it could be either motion cues from the female or the male's own motor state governing vibration output.

By controlling female speed combined with statistical modeling, we show that it is locomotion cues informing the male to select vibration production over song.

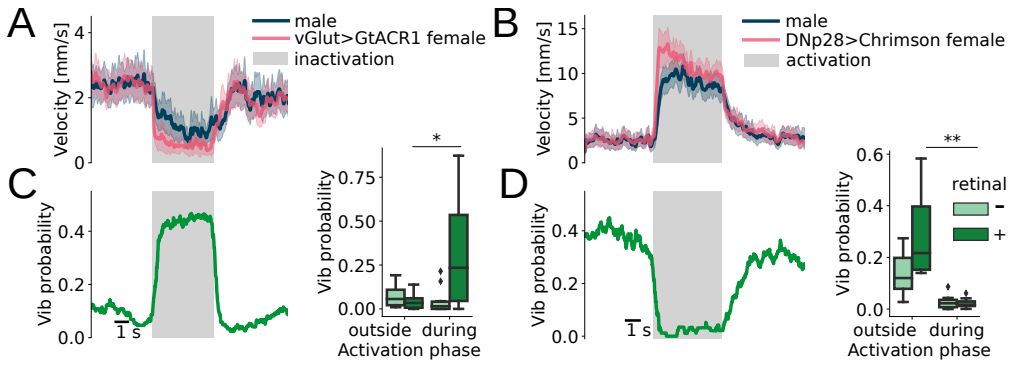

Figure 3: **Female immobility is a necessary and sufficient trigger for male vibrations.** **A** vGlut inactivation induces female immobility and triggers male vibration production. Velocity magnitude traces of male (blue) and female (pink) around optogenetic inactivation stimulus. **C** The corresponding vibration probability trace (left). Vibration probability (right) during (control 0.01 ± 0.07, retinal 0.23 ± 0.29) or outside (control 0.06 ± 0.06, retinal 0.03 ± 0.04) optogenetic inactivation for experimental flies and non-retinal control, p = 0.0012, one-sided paired t-test, significance level corrected to p = 0.005 by Bonferroni as we also tested effects on song types. **B** DNp28 activation induces female forward walking and triggers a stop in male vibration production. Velocity magnitude traces (top) of male (blue) and female (pink) around optogenetic activation stimulus. **D** The corresponding vibration probability trace (left). Vibration probability (right) during (control 0.02 ± 0.03, retinal 0.02 ± 0.02) or outside (control 0.12 ± 0.08, retinal 0.22 ± 0.15) optogenetic activation, p = 0.0008, one-sided paired t-test, significance level corrected to p = 0.005 by Bonferroni as we also tested effects on song types (data not shown).

3.3 TWO CENTRAL NEURON CLUSTERS CONTROL SONG AND VIBRATION PRODUCTION WITH OPPOSING DYNAMICS

3.3.1 *Song and vibration output are tightly integrated in the central brain*

Up to now, we showed that song and vibration are distinct signal types which are chosen by the male in a defined social context. Next, we wanted to find how and where the signal choice is neuronally controlled. Neurons controlling a signal choice would ideally integrate information from several social cues but also drive behavioral command neurons. Two neuron clusters driving song production in solitary males are the sexually dimorphic pC2l and P1a (Deutsch et al. 2019; Roemschied et al. 2021; Clemens et al. 2018; Roemschied et al. 2021). Both integrate different cues in courtship (Deutsch et al. 2019; Kohatsu and Yamamoto 2015; Clowney et al. 2015; Kallman, Kim, and Scott 2015) and pC2l has been shown to be anatomically and functionally upstream of pIP10 (Lillvis et al. 2022; Roemschied et al. 2021), a descending song neuron (Philipsborn et al. 2011; Ding et al. 2019). Vibration production has been linked to two broad neuron populations controlling courtship behavior: *doublesex* and *fruitless* (Fabre et al. 2012). However, narrower neuron clusters driving vibrations have not been specified yet.

Asking, if there are distinct central drivers for song and vibration, we optogenetically activated pC2l and P1a in solitary males (Figure 4A). In case of a separate central control for both signals, pC2l or P1a would be determined to only drive song. A central integration of signal choice would interlink the output of both signals. To our surprise, we found that both pC2l and P1a drive not only song but also vibration production (Figure

4C-F). We concluded that the production of both courtship signals is tightly integrated in the central brain.

The tight central integration of courtship signal control suggests that pC2l and P1a are part of the same circuit. Within such a circuit, connectivity and physiological properties will result in intrinsic dynamics when activating circuit nodes such as pC2l or P1a. Activating either neuron cluster, in the absence of additional cues, could therefore yield a stereotypical (preserved) pattern (order) of signal generation. Inspecting the pattern of signal output, we indeed found that pC2l and P1a control song and vibration production with distinct dynamics. When activating pC2l (R42B01 ∩ *doublesex*) in solitary males, the males sang pulse song during optogenetic stimulation which was often followed by vibration generation after stimulation (Figure 4C,E). pC2l has been described to show an offset response for sine song after pulse production for similar activation intensities but shorter activation durations than we used. These sine offsets are 1-2 s long and therefore shorter than the vibration offset we observe (Roemschied et al. 2021).

Activating P1a (R71G01 ∩ R15A01) in solitary males showed opposing dynamics: P1a reliably induced vibrations during stimulation. After stimulation, most males continued to vibrate while some would start singing courtship song (Figure 4D,F). P1a gates persistent courtship displays in the male, however P1a activity has hardly been linked to a specific and acute behavior. In line with our finding, optogenetic P1a stimulation was described before to induce "extended periods of locomotor arrest" (Hoopfer et al. 2015). Vibrating male flies are immobile when observed from above. To our knowledge, we are the first ones to show with vibration production a direct and reliable output of P1a. We observed that vibration production of the male coincided with immobility (Figure 4H), suggesting that his stopping is part of the vibration motor program. Opposingly, when activating pC2l, we found a trend that males sped up during the optogenetic stimulation (Figure 4G).

With pC2l and P1a we found two nodes of a courtship signal circuit: pC2l directly drives pulse song whereas the other node P1a directly drives vibration. Both neurons indirectly drive the other signal after activation, respectively, and P1a shows additional persistent dynamics. This demonstrates that the production of both signals is tightly integrated in the central brain. The intrinsic dynamics of the signal selecting circuit drive complex and persistent behavioral patterns.

3.3.2 *A circuit model for dynamics*

What kind of circuit could implement the observed dynamics? We hypothesized the following circuit: pC2l is functionally upstream of P1a (previously suggested by Roemschied et al. 2021). When activated, either cluster drives song or vibration directly via a descending node. Mutual inhibition between the descending output pathways reduces the overlap between both signal types. pC2l drives P1a, which results in the vibration offset after pC2l activation. Sufficient P1a activity additionally drives a persistence node that maintains vibration and song production even in the absence of sensory cues (Figure 4B).

In our model pC2l drives song by activating the descending neuron pIP10 (Philipsborn et al. 2011; Roemschied et al. 2021). Similarly, P1a drives vibrations via a descending neu-

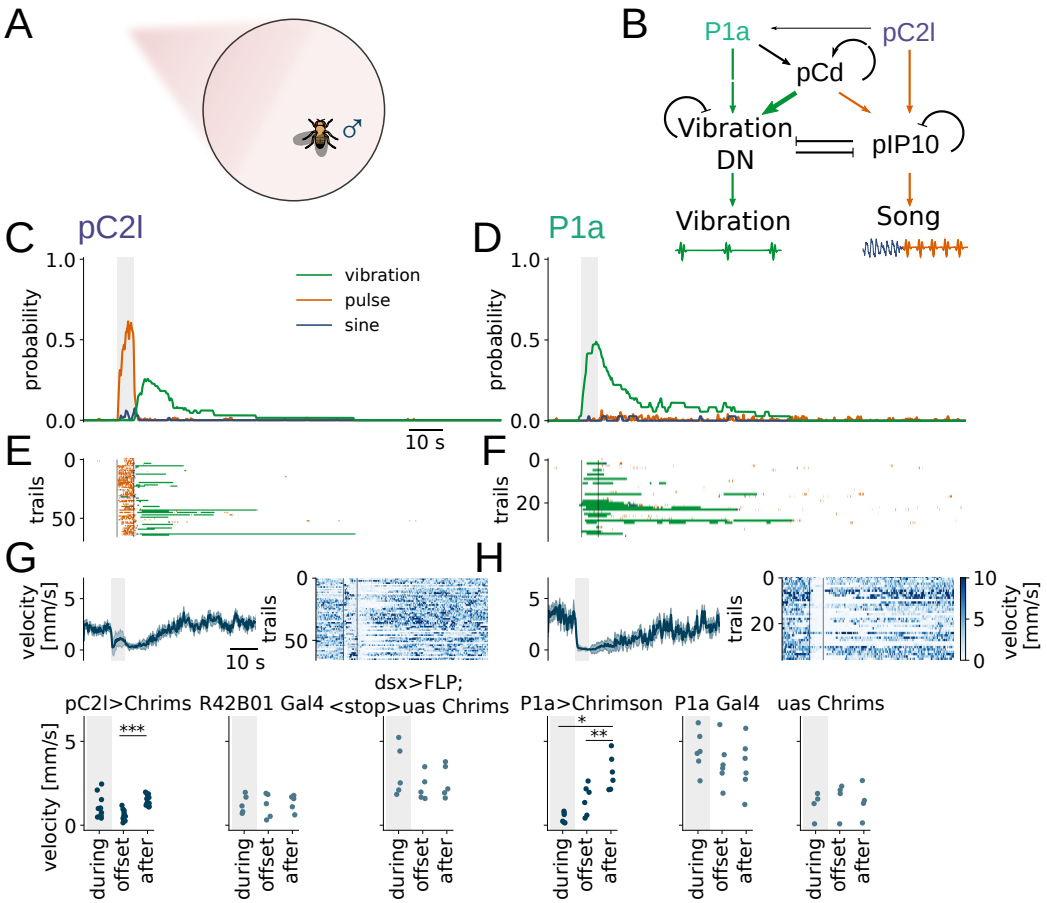

Figure 4: **P1a and pC2l control vibration and song with intrinsic dynamics.**
A Schematic of solitary male in behavioral chamber for optogenetic activation of pC2l or P1a neurons. **B** Circuit model of signal pathway based on optogenetic activation results and literature: pC2l and P1a drive a descending song and vibration output, respectively. pC2l drived vibrations via P1a. P1a activates a persistency node. Mutual inhibition between both output pathways limits the output to one signal type. **C-D** Average pulse, sine and vibration probability trace around optogenetic activation of pC2l (**C**) and P1a (**D**). **E-F** Single trial signal traces underlying the averages in (**C-D**). **G-H** Average trace (left), single trial data (right) and quantification (bottom) of male velocity magnitude around optogenetic activation (left), thick line: median, shading: sem; for pC2l (**G**) and P1a (**H**) activation respectively. On the bottom velocity modulation during optogenetic activation, at offset (until 15 s after offset) and after offset (15 s after stimulus stop until end of trial) are quantified for experimental flies and optogenetic controls. Only experimental flies show velocity modulation (pC2l > Chrimson between offset and after $p = 1 \times 10^{-5}$; and P1a > Chrimson between during and after p = 0.0017; and between offset and after p = 0.0006; paired t-test, significance level corrected to p = 0.0028 by Bonferroni). Data in C-F shown for P1a n = 6 flies and pC2l n = 11, n = 6 trials per fly.

ron. The persistent vibrations and song result from a recurrent neural network downstream of P1a (potentially pCd, Jung et al. 2020) that maintains a courtship state in the absence of sensory cues. Mutual inhibition between the descending neurons reduces the overlap between both signal types. Both descending neurons adapt with time, which allows the other signal pathway to drive the alternative output (Figure 4B).

3.4 COURTSHIP DRIVE SHAPES CIRCUIT DYNAMICS AT INTERMEDIATE TIMESCALES

When we activated P1a in solitary males, we observed persistent vibration production in males which outlasted the stimulation time and would sometimes continue for minutes (Figure 4D and 5C). Similarly, pC2l drove vibrations after activation, but much shorter (Figure 4C and 5B). These findings match with previously observed neuronal effects controlling courtship motivation on two timescales. On a shorter timescale P1 activity outlasts stimulation for 5-10 s (Inagaki et al. 2014; Zhang, Miner, et al. 2018, but much longer when stimulated longer: Hoopfer et al. 2015) but also induces a longer lasting courtship drive (from minutes to days) by recruiting other neuron populations which maintain the arousal state (Jung et al. 2020; Zhang, Rogulja, and Crickmore 2019; Zhang, Miner, et al. 2018).

To test how courtship drive would affect the dynamics of our circuit, we performed a satiety assay. Males were allowed to court females freely before the experiment, then we activated pC2l or P1a and inspected the effect of reduced courtship drive on the signal output of either neuron cluster (Figure 5A).

Upon pC2l activation we found that sexual satiation completely abolished the vibration offset response, whereas pulse song production during optogenetic stimulation was unaffected (Figure 5B,D). Consulting our model, we inferred that stimulating pC2l in males with low courtship drive still led to singing but that satiation decreased P1a excitability and therefore abolished the P1a mediated vibration output afterwards.

Next, we activated P1a in satiated males. A reduction in courtship drive drastically shortened the persistence phase upon P1a stimulation, song and vibration output were completely abolished after 9 s. In contrast, vibration production during optogenetic activation was unaffected (Figure 5C,E). This suggests that P1a drives vibrations via two pathways: a direct one during P1a activation, and an indirect one after P1a activation. A likely candidate to drive a persistent social behavior is the neuron cluster pCd. pCd is required for persistent singing and functionally downstream of P1a (Jung et al. 2020). Sexual satiety was shown to downregulate pCd and subsequently to decrease persistent social behavior (Zhang, Rogulja, and Crickmore 2019).

Satiating the male's courtship motivation coincides with faster decay of P1 activity reduced and pCd excitability (Zhang, Miner, et al. 2018; Zhang, Rogulja, and Crickmore 2019). A reduction in courtship drive affected the intrinsic dynamics of our circuit on two time scales. We suggest that a decreased excitability of P1a as a downstream target of pC2l reduced the complexity of behavioral output by abolishing the vibration offset within the first seconds after pC2l activity. We further hypothesize that the combination of decreased P1a and pCd activity lowered the persistence of the circuits output after P1a activity, on a scale of minutes.

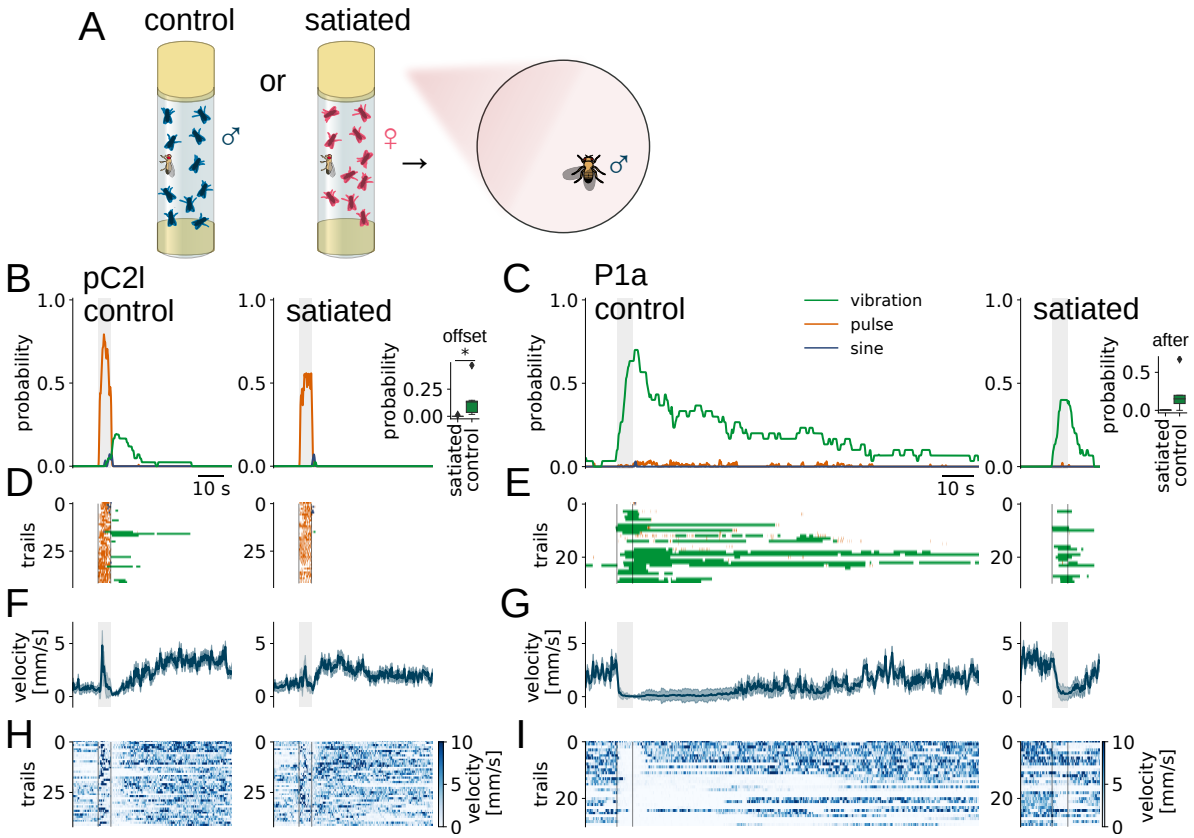

Figure 5: **Internal state modulates dynamics by which P1a and pC2l control signals.** **A** Schematic illustrating satiation assay. Group-housed males single males were pre-incubated in vial with 10-15 virgins or males (control) for 4-6 hours. Subsequently, a pre-incubated solitary male were placed in behavioral chamber for optogenetic activation of pC2l or P1a. **B-C** Average pulse, sine and vibration probability trace around optogenetic activation of pC2l for sexually satiated males (right) and controls (left), same for P1a (**C**). **B** Inlet compares the vibration probability at stimulation offset (end of stimulus until 15 s later) between both groups (satiated 0.00 $\pm$ 0.00 and control 0.13 $\pm$ 0.14; median $\pm$ std), p = 0.039, t-test, n = 7 flies per condition, n = 6 trial per fly. **C** Inlet compares the vibration probability after optogenetic stimulation (end of stimulus until end of trial) between both groups (satiated 0.001 $\pm$ 0.003 and control 0.15 $\pm$ 0.23; median $\pm$ std), p = 0.099, t-test, n = 5 flies per condition, n = 6 trials per fly. **D-E** Single trial signal traces underlying the averages in (**B-C**). **F-G** Average trace of male velocity magnitude around optogenetic activation, thick line: median, shading: sem; for pC2l (**F**) and P1a (**G**) activation in satiated (right) and control males (left), respectively. **H-I** Single trial data of male velocity magnitude around optogenetic activation underlying traces in **F-G**.

3.5 SOCIAL CUES MODULATE CIRCUIT DYNAMICS

Above we showed that social context is crucial to select the appropriate communication signal and that intrinsic circuit dynamics drive complex and persistent behavioral patterns even in absence of context-defining cues. But for a signal selecting circuit to support context-dependent signaling, it should be modulatable by sensory cues. To test how sensory cues modify the intrinsic circuit dynamics, we stimulated pC2l and P1a in the presence of a female (Figure 6A and 7A). Two extreme assumptions would be that the circuit is either blind to the social cues or that the social cues completely overwrite circuit dynamics. Stimulating neurons in a cue blind circuit would interrupt the ongoing courtship signal patterning and yield a similar output as observed in a single male, after a phase of adaptation he may resume courting. If the cues simply overwrite circuit dynamics, the male would just continue to court irrespective of neuronal stimulation.

When stimulating pC2l in a presence of a female we found that the males still sang pulse song during the time of stimulation and stopped producing vibrations and most sine song (Figure 6B-C). This suggests that regardless of cues, pC2l activity will drive pulse song and inhibit the vibration output at the same time. pC2l in single males drove a vibration rebound after stimulation with almost absent song production (Figure 4C). In the presence of a female we loose the pronounced vibration rebound with absence of song. Instead, after pC2l stimulation, the males closed their wings for a short moment (Figure 6E) but quickly start to sing or vibrate again (Figure 6B). In the majority of cases the male will return to the signal type he produced before pC2l activation, with the exception of sine song. Males who sang sine song before pC2l activation will always switch to pulse or vibration after the pC2l activation (Figure 6F). Notably, a quick wing closure and stop of pulse song right after pC2l activation is still indicative for brief P1a activity. The presence of the female cues however quickly allow the male to produce signals context-accordingly. This suggests that the direct output of pC2l – that is song production and vibration inhibition – is agnostic to social cues. But that the downstream effects – that is recruiting P1a with vibration rebound for 15 s – are quickly modulated by social cues.

When stimulating P1a in the presence of a female, the male still vibrated but stopped singing during stimulation (Figure 7B-C). The loss in song production during optogenetic stimulation is accompanied by wing closure (Figure 7E). Whenever the males vibrated during stimulation, these vibration were correlated with low velocities of male and female (Figure 7C, right). This suggests that P1a activity will allow for vibration production but only in the correct context, that is when the female is stationary. The circuits effect of inhibiting song output during P1a stimulation remains regardless of social cues. P1a in solitary males mainly drove persistent vibrations after stimulation and sometimes song production (Figure 4D). In the presence of a female we no longer observe such a persistent signal preference. Instead, after optogenetic stimulation, the males sing or vibrate at baseline level.

We conclude that the direct output of P1a – that is vibration production and song inhibition – is agnostic to social cues. But that the downstream effects – that is persistent vibration generation – are quickly modulated by social cues.

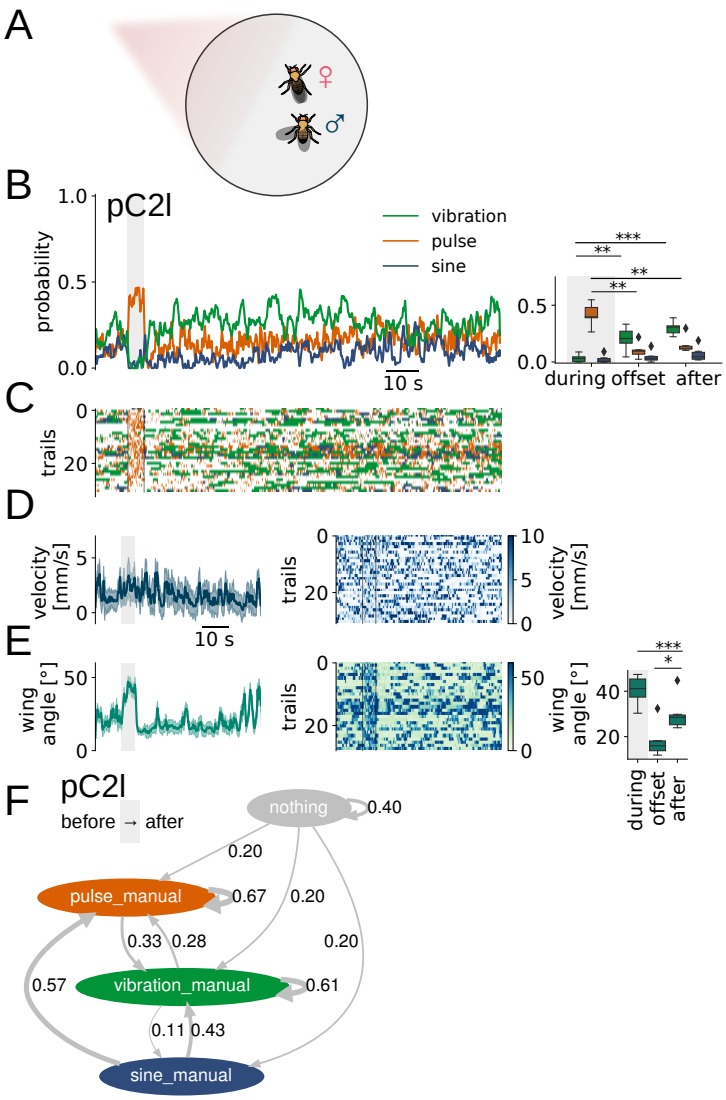

Figure 6: **Social cues quickly overwrite downstream effects of pC2l signal control.** **A** Schematic illustrating female derived social cue assay. Group-housed solitary males were introduced to single virgin female in behavioral chamber for optogenetic activation of pC2l. **B** Average pulse, sine and vibration probability trace (left) around optogenetic activation of pC2l for male courting a female. Quantified (right) are the signal type probability during stimulus, at stimulation offset (end of stimulus until 15 s later) and after offset (until end of trial) showing that pulse probability during pC2l stimulation is increased (during 0.40 $\pm$ 0.09, offset 0.09 $\pm$ 0.06 with p = 0.001, after 0.12 $\pm$ 0.07 with p = 0.001, paired t-test) and vibration probability decreased (during 0.03 $\pm$ 0.03, offset 0.21 $\pm$ 0.09 with p = 0.007, after 0.31 $\pm$ 0.05 with p = 5 x 10^{-5}, paired t-test). **C** Single trial signal traces underlying the averages in **B**. **D** Average trace (left) and single trial data (right) of male velocity magnitude around optogenetic activation (left), thick line: median, shading: sem. **E** Average trace (left) and single trial data (middle) of male wing angle sum around optogenetic activation, thick line: median, shading: sem. Quantified (right) are the male wing angle sum during (41° $\pm$ 6) and right after stimulus offset (16° $\pm$ 7, 0.6 s until 2.6 s after stimulus offset, p = 0.0003, paired t-test) and after offset (29° $\pm$ 7, 15 s after offset until end of trial, p = 0.01) optogenetic stimulation. The male's wings are extended during and briefly close after pC2l stimulation. For pC2l n = 6 flies, with n = 6 trials per fly. **F** Transition between signal types before and after stimulation. Indicating the most probable signal type in the 5 s before and after the optogenetic activation of pC2l.

Activating P1a in solitary males resulted not only in vibration generation but also in male immobility (Figure 4H). To our surprise, in the presence of a female, we loose this effect on male walking (Figure 7D). We inferred that female cues are the sufficient trigger for a male's walking behavior which in turn gates a vibration command from P1a, potentially via ascending neurons (Chen, Aymanns, et al. 2022).

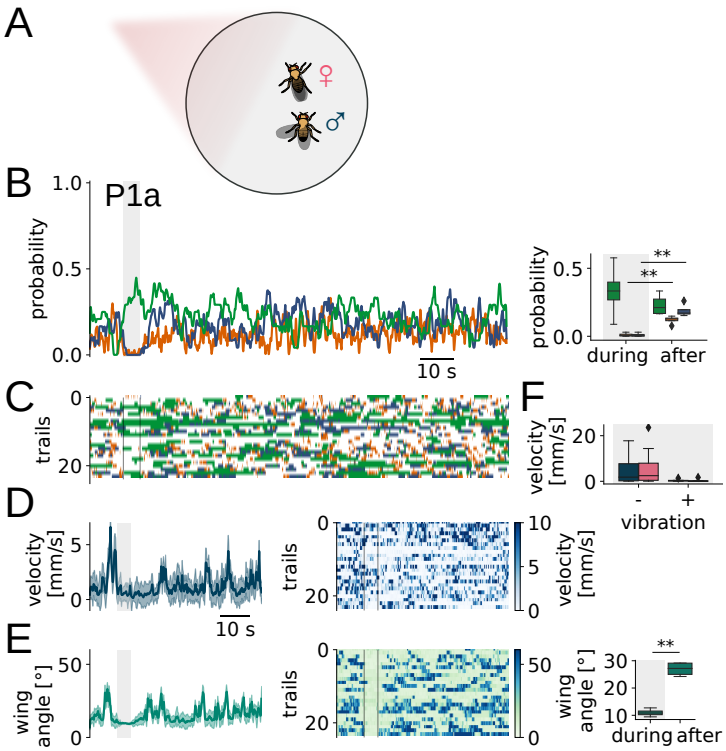

Figure 7: **Song inhibition by P1a is agnostic to social cues.**
A Schematic illustrating female derived social cue assay. Group-housed solitary males were introduced to single virgin female in behavioral chamber for optogenetic activation of P1a. **B** Average pulse, sine and vibration probability trace (left) around optogenetic activation of P1a in males courting a female. Quantified (right) are the signal probabilities during and after optogenetic stimulation showing that sine and pulse song are decreased during P1a stimulation (pulse 0.006 $\pm$ 0.012, sine 0.004 $\pm$ 0.012) compared to after (pulse 0.13 $\pm$ 0.03, p = 0.004, sine 0.17 $\pm$ 0.04, p = 0.002), paired t-test. **C** Single trial signal traces underlying the averages in **B**. **D** Average trace (left) and single trial data (right) of male velocity magnitude around optogenetic activation (left), thick line: median, shading: sem. **E** Average trace (left) and single trial data (middle) of male wing angle sum around optogenetic activation, thick line: median, shading: sem. Quantified (right) are the male wing angle sum during (11° $\pm$ 1) and after (27° $\pm$ 2) optogenetic stimulation showing that the male's wings are closed during P1a stimulation, p = 0.002, paired t-test. Data for P1a are n = 4 flies, with n = 6 trials per fly. **F** Quantified are male and female velocity magnitude during optogenetic stimulation for trials in which the male vibrated (male 0.25 mm/s $\pm$ 0.43 and female 0.13 mm/s $\pm$ 0.57) or did not (male 1.82 mm/s $\pm$ 4.75 and female 2.47 mm/s $\pm$ 6.33). Velocities are low when male vibrates but not significantly different to the condition without vibration (male velocity p = 0.06, female velocity p = 0.07, t-test).

4

DISCUSSION

4.1 VIBRATIONS, AN OVERLOOKED COURTSHIP COMMUNICATION SIGNAL

In behavioral research, we are at risk to miss important observations and subsequently misinterpret phenomena. To draw a complete picture of social interaction, it is of advantage to exhaustively quantify the behavior of the involved individuals. By lacking readouts of communicative channels, insufficient data resolution or just the wrong video recording angle, vibration signalling became a highly overlooked aspect of *Drosophila* courtship. Although it is the most prevalent courtship signal (Figure 1E), most publications on *Drosophila melanogaster* courtship communication deal with courtship song and only few with vibration signals (Fabre et al. 2012; McKelvey et al. 2021; Hernández and Fabre 2016; Mazzoni, Anfora, and Virant-Doberlet 2013). Furthermore, knowledge of the behavioral context of vibrations offers explanations for previously described phenomena. When recording *Drosophila* courtship with low spacial resolution from the top, a vibrating male appears like a male who does nothing, just standing close to the female. Such an observation, without the corresponding audio traces that reveal the real communicative content of this situation, easily lead to the misconception that the male takes long pauses in courtship. This fact often left researchers puzzled about some observations when activating P1a for instance. Hoopfer et al. 2015 describe a male motor arrest upon P1a activation, Roemschied et al. 2021 find that at similar optogenetic activation intensities as we use (1, 25, 205 $\mu W/mm^2$), P1a hardly drives any courtship song. Calhoun, Pillow, and Murthy 2019 found three internal states to govern courtship signalling, one of them being the "Whatever" state. Examining the behavioural cues defining the "Whatever" state and the corresponding signal output, quickly allows to infer that this state, in reality, is a vibration state. Male flies in this state hardly sing, the transition to the "Whatever" state is linked to a reduction in male and female speed and a larger distance between them. All of these correlations define the vibration context in our study. With this thesis we can fill these gaps in interpretation by showing that the male in fact is communicating to the female with vibrations during such putative courtship pauses.

4.2 THE ULTIMATE AND PROXIMATE WHY OF VIBRATIONS.

The ultimate why asks why a behavior exists, addressing its evolutionary function. The proximate why is concerned with the mechanism responsible for a behavior (Mayr 1961). First possible reasons of evolution or females to select vibrating males will be discussed and afterwards how a male mechanistically generates vibrations.

4.2.1 *Why is vibration signalling ultimately selected?*

What is the evolutionary function of vibration signals, or how we call it: why-brate in the first place? A number of reasonable explanations why vibrating males evolved or are preferred by females are discussed below. To give an overview, we will address the following aspects: Vibrations are an additional communication modality and could hereby compensate for other communication channels. They could serve as an honest signal and demonstrate a male's fitness. They may be less costly for the male; an energy saving signal. Vibration signals could inform a female about behavioral context or substrate quality. They may reinforce species differentiation and be less prone for eavesdropping.

First of all, vibrations add an additional modality to the courtship signal repertoire of a male. While song is transmitted through the air, vibrations are transmitted through the substrate. Such an additional communication channel is an advantage in case of wind which may distort air-borne signals, when the courted female has damaged aristae and cannot pick up song or when a male has damaged wings and cannot generate song. It was reported before that wing-cut males vibrate more (Fabre et al. 2012), suggesting that they compensate the lack of song with vibrations, though we could not reproduce this effect (Figure 1.2F).

Furthermore, courtship song was suggested to serve as an honest signal (Swain and Philipsborn 2021) and this can be similarly argued for vibrations. By producing *good vibrations* (that is with the right IPI and pulse shape) and in the appropriate context, the male may demonstrate his fitness. For signal production he needs to neurally orchestrate and thereafter engage the generating muscles and body parts. By patterning his signals according to context, he shows that his senses inform him correctly about current conditions and yield an accurate output. However, for this argumentation to hold, vibrations need to affect male mating success which was implied before but has never been tested directly (McKelvey et al. 2021). Two testing strategies could show such an effect: first vibration playback could increase copulation rates and frequencies and second diminishing vibrations from the courtship ritual, by preventing males to generate them or introducing the couple to a non-vibratory substrate could reduce copulation success. Conversely, a boost in male mating success was shown for pulse song but never for sine song (Rybak et al. 2002), pointing to the idea that not all courtship signals have an explicit impact on mating success. Here, more subtle readouts of female receptivity, like slowing, longer stretches of immobility, vaginal plate opening or abdominal grooming indicate her preference for vibrations.

Moreover, vibrations may be a less costly signal than pulse or sine song because their pulses are spaced much wider and the male stands still during their production. At the same time, he still communicates to the female, that he is close and courting her while potentially saving energy by vibrating instead of singing. Knowledge of the number and size of involved muscles for vibration versus song generation could already suggest such a function. More directly, expression of a fluorescent adenosine 5'-triphosphate (ATP) sensor in muscles would allow to measure the energy consumption during either signal output (Tsuyama et al. 2013). Another possibility is to measure the metabolic rate during either signal output, however when using chambers to detect O_2 consumption

or CO_2 production (Voorhies 2009), it will be challenging to control the time points of song and vibration generation.

Why would a male would prefer to vibrate as opposed to attempting copulation once a female has stopped walking? A copulation attempt may require an additional trigger, like vaginal plate opening or ovipositor extrusion which were shown to precede copulation attempts in males (Mezzera et al. 2020; Wang et al. 2021). One could test this by optogenetically inducing vaginal plate openings in females and quantify how likely they trigger a copulation attempt in a vibrating male.

Another plausible explanation for why male vibration signalling developed is that vibrations could provide relevant information about the current context to the female. If the male was to produce signals randomly, without regard to current conditions, the female would gain no new information by attending to his signals. But because vibration generation is linked to male immobility, she could infer the male's motor state, that he is standing near her, maybe even where he is if she can infer his position from comparing when vibration pulses reach which of her legs. Considering that vibrations are transmitted on different fruit surfaces (McKelvey et al. 2021) and that females prefer to mate in a rich nutritional environment (Gorter et al. 2016), vibrations could even inform the female about the quality of the substrate for future egg deposition. All of these female interpretations of vibrations are difficult to test. Taking it step by step, we could trace vibration processing in the female from mechanosensory neurons in the ventral nerve cord, to the AMMC and to higher brain centers. Functional calcium imaging in selected neuron populations, like neurons expressing the sex determination genes *fruitless* or *doublesex* or imaging panneuronally while exposing the female to vibration playback would reveal the path of vibration processing. If responses to vibration signals are processed in similar centers as for example egg deposition choices, this would at least point to their potential role in substrate evaluation. Furthermore, by changing playback parameters, we could functionally map the mechanosensory features that female brains are tuned to. This would also enable the search for direction selective neurons, hinting to the role of vibrations in providing location information about the male. A location informing role could also be tested behaviorally by playing vibrations from a precise source and probe for effects on female behavior, like a bias in direction of walking initiation.

Vibrations signals could also allow for species differentiation because other *Drosophila* species were shown to have a shorter IPI than *Drosophila melanogaster* (Figure 1F, Hernández and Fabre 2016). Playback of vibrations with varying IPI and comparing their effect on receptivity in females from different species would reveal such species-specific preference for vibration IPIs. In other insects, like katydids or crickets, vibrational signals attract the female to the location of the male (Morris and Luca 1998; Weidemann and Keuper 1987; Stritih-Peljhan and Virant-Doberlet 2021) but in case of *Drosophila* they are rather a close-proximity signal (Figure 2.1A,D-E).

Finally, substrate-borne vibrations may be less prone to eavesdropping by other males or predators. The detection of vibration signals requires another male or predator to be on the same substrate and walking of the eves dropper probably distorts or interferes with vibration detection. In contrast, courtship song is heard by nearby males and has been shown to reinforce courtship behavior in them (Li, Ishimoto, and Kamikouchi 2018;

Zhou et al. 2015; Yoon et al. 2013). If vibrations also provoke male courtship arousal in a similar manner as song, vibration playback experiments should enhance male-male courtship, speed up courtship initiation of males and trigger an increase in male speed. However, the absence of such effects would support the hypothesis that vibrations ensure a rather private communication channel between the male and the immobile female in front of him.

To sum up, there are several plausible reasons for the ultimate why evolution or females selected vibrating males and we suggested testing strategies to probe them.

4.2.2 *Vibration generation downstream of P1a*

The proximate why is concerned with the mechanism how males generate vibrations. This addresses all levels of vibration production: body parts, muscles, motor neurons and central control. We showed that vibrations are neither generated with the male's wings nor by their abdominal quivering (as previously suggested Fabre et al. 2012, Figure 1.2). However, which body part, muscles or motor neurons are involved in their production remains elusive. We hypothesize that vibrations are generated by muscles in the male's thorax. The thorax houses multiple muscles which generate sufficient force for e.g. flight or wing movement in courtship song (O'Sullivan et al. 2018). As the thorax lies directly on top of the male's legs, it is a plausible assumption that force originating from the thorax could be transmitted through the legs to the substrate for vibration generation.

Is there an overlap between muscles involved in song production and vibration production or are those two completely independent motor programs? Our observation that males are able to generate sine song and vibrations at the same time (although this is rarely the case, Figure 1.3A) indicates that at least muscles for sine and vibration generation are distinct. In contrast to that, the waveforms of pulse song and vibrations highly resemble each other (Figure 1.1C, Clemens et al. 2018) , suggesting that similar motor programs could be involved in their generation. An easy way to test this hypothesis would be to silence motor neurons known to shape acoustic parameters of pulse song (O'Sullivan et al. 2018) and test for similar effects on vibration signals. Determining the motor neurons generating vibrations would further guide the search for a descending neuron or vibration command neuron. Such a descending neuron is likely to terminate in the same VNC neuropil where also the vibration motor neurons lie. pIP10 for example terminates in the wing neuropil, the wing neuropil is also innervated by song shaping motor neurons (O'Sullivan et al. 2018, Philipsborn et al. 2011). In case of direct synaptic contact between the motor neurons and a descending neuron, anatomical retrograde tracing tools in Drosophila such as BAcTrace (Cachero, Gkantia, et al. 2020) or *retro*-Tango (Sorkaç et al. 2022) could reveal the descending neuron's shape. Similarly, direct connectivity could enable the search for this descending neuron in the soon to be published male's VNC connectome (Phelps et al. 2021), making the search for a driver line easier. The next steps for probing the vibration-song-coordinating circuit would be first to determine if P1a is directly upstream of the vibration descending neuron and second to identify the pattern generators targeted by this descending neuron.

With P1a we already found one answer to the question "why do males vibrate – proximately?": because P1a neurons are active and their activity is sufficient to trigger vibration production in a male. Finding how vibrations are controlled and generated downstream of P1a, will contribute to the fundamental understanding of motor coordination in signal control, behavioral command execution and action selection circuits.

Asking about the ultimate and proximate why of vibrations connects different fields of research. The ultimate question is relevant in evolution and ecology studies whereas the proximate basis of vibrations would be investigated more narrowly in neuroscience. The complex social behavior of *Drosophila* and its genetic tools for manipulating and monitoring neural activity pave the way for such interdisciplinary questions.

4.3 BEHAVIORAL MODULATION BY EXTERNAL CUES AND INTERNAL STATES

Social communication is a flexible behavior which animals need to adapt to internal changes or changes in the environment. Accordingly, communication signal selection is modulated by internal and external cues. Internal changes involve overall internal states but also behavioral states (Devineni and Scaplen 2022). Whereas internal states reflect basic needs of a fly, like a drive for foraging induced by hunger or a high courtship motivation due to lack of recent mating, behavioral states modulate how a sensory stimulus is transformed into a behavioral response on a moment-to-moment basis. Depending on whether a fly is walking, flying, or immobile, the salience or meaning of sensory input varies. Behavioral states therefore introduce flexibility to behavior by adjusting sensorimotor transformations, modulating sensory processing or motor responses (Devineni and Scaplen 2022; Calhoun, Pillow, and Murthy 2019).

External cues shaping the male's communication behavior involve prior experience and environmental context. Context is inferred by the male's actual sensory experience.

In the behavioral experiments and analysis of wild-type males presented in this thesis, internal state and prior experience were controlled for. We tested well-fed, sexually naive, group-housed males of similar age at their morning activity peak. This is why this discussion focuses on external sensory cues and behavioral motor states guiding signal selection.

4.3.1 *Sensory cues guiding signal selection*

Our analyses of fly behavioral cues combined with computational modelling and tested with optogenetics (Figures 2-3) showed that signal selection is context-dependent. The male sings when he is close to the female (Figure 2.1A,D-E) and he vibrates when she, and subsequently he stops moving (Figure 3A,C). But which sensory cues inform him about the current context? A stop and start in movement, which trigger the onset and offset of vibration production in him, could be detected by visual, mechanosensory or potentially olfactory cues. To test, if visual cues inform him, we could examine couples in the dark or blind courting males and quantify if the amount of produced vibrations changes or the context for their occurrence is less defined. If the complete absence of vi-

sual cues yields an effect, we could pinpoint this effect further, probing different motion detectors in the visual system (Strother et al. 2017) or higher visual projection neurons that convey courtship-relevant information (LC neurons, Ribeiro et al. 2018; McKinney and Ben-Shahar 2019). Alternatively, we could test a male on a treadmill, set him in a courtship state by activating P1a (Hindmarsh Sten et al. 2021) and trigger his signal choice by controlling his visual input. Such a setup would even allow us to extract which visual features drive vibration onset or offset. In contrast to testing the role of visual cues, testing if mechanosensory cues inform his signal choice is more challenging. We could induce substrate movement or introduce the couple to a substrate that does not transmit walking-induced deflections. However, inducing movement would likely interfere with vibration recordings and would have to be fine tuned to avoid startle responses of male and female. Introducing the couple to a non-transmitting substrate would additionally prevent vibrations to reach the female. Finally, silencing mechanosensory neurons in males likely interferes with their walking behavior because mechanosensors also provide proprioceptive feedback (Mendes et al. 2013). To test if olfactory cues are necessary for context-appropriate vibration production, we could test smell blind males (Larsson et al. 2004; Coen et al. 2014). Although olfactory cues were suggested to provide positional information in courtship (Taisz et al. 2022), they are not very precise for detecting movement of a target because they are easily disrupted by wind or other nearby flies. Moreover, courtship usually happens on fruit in the wild, where plenty of other flies from the same or another species are around (Dukas 2020). In a natural setting, cues derived from walking sound, substrate deflections or changes in olfactory intensity could originate from any other fly in proximity. Visual cues, in contrast allow for better target-oriented detection of movement.

In line with the idea that it is predominantly visual cues guiding his signal selection, are findings that the absence of visual cues affects courtship song patterning (Coen et al. 2014). Visually impaired males (blind, with silenced motion detectors or silenced LC10 neurons which support visual courtship pursuit) have pronounced courtship deficits, their ability to orient toward or stay close the the female are strongly reduced (Ribeiro et al. 2018).

Finally, a male decides to continue vibrating if the female remains stationary, resulting in relatively long vibration trains (Figure 1C,G). Her immobility is reflected by the absence of changes in cues. An internal arousal state of the male, a stable visual target in front of him and non-changing olfactory input should be sufficient to maintain vibration output. Considering that P1a encodes sexual arousal in a male (Hindmarsh Sten et al. 2021) and is stimulated by pheromonal cues (Clowney et al. 2015; Kallman, Kim, and Scott 2015), it makes sense that activating P1a in absence of other cues triggers vibration output in solitary males (Figure 4D).

To conclude, visual cues likely inform the male when to produce song and when vibrations and probably guide his switching between courtship communication signals.

4.3.2 *The link between signal output and male motor state*

Above we discussed which sensory cues guide the male in adapting his communication behavior to environmental context. But also internal changes, like different locomotor states, shape a male's signal output. There is a cross-talk of locomotor and neural activity which goes both ways: neurons can trigger a defined motor program but also physical activity may increase arousal or a certain posture could inhibit other movements. When we examined the natural context of vibration production (Figures 2.1B and 2.2A (right)) or artificially induced vibration generation in solitary males (Figure 4H), vibrations and male immobility typically coincided. In the presence of a female, P1a activation still triggered vibrations but only in situations when he and she were standing still (Figure 7C (right)). This suggests that first the vibration motor program includes immobility and second that it is probably the male's motor state gating vibration output. On top of that, artificially activating P1a resulted in wing closure of a courting male (Figure 7E), suggesting that the vibration motor program does not only include immobility but also wing closure. However, the effect of P1a to close the male's wings seems to depend on the tool of activation and activation length and intensity, as other studies report wing extensions or song production upon P1a activation in solitary males (Hoopfer et al. 2015; Jung et al. 2020; Clemens et al. 2018). If immobility and wing closure are part of the vibration motor program, motor neurons for leg and wing movement are either inhibited during vibrations or all together under tonic tension holding the standing/closed posture. Calcium imaging of muscle groups active in vibration production would reveal which muscles are rhytmically active O'Sullivan et al. 2018, presumably driving the vibrations and which are tonically active, shaping additional posture features such as standing or wing closure. The identification of a vibration descending neuron would allow to find downstream motor neurons and a link of immobility and wing closure to the vibration command.

How could the male's motor state gate vibration output? Motor state could be encoded by proprioceptive feedback or a copy of locomotor commands. Whereas self-motion and proprioceptive feedback is conveyed by ascending neurons, an efference copy by an immobility descending neuron could similarly gate vibration output. A testing strategy would be to activate ascending neurons to mimic a male's current standing posture or mechanically prevent him from moving (Chen, Aymanns, et al. 2022). Such a trigger could gate vibration output in a courting or sexually aroused male. Similarly, making a male stationary by activating an immobility descending neuron may bias a courting male to vibrate.

Previous work on *Drosophila* courtship song found that three distinct behavioral states in a courting male govern his sensorimotor strategies to select between song types. We propose that the third state they find, the "Whatever" state in which males rarely sing and both flies show reduced speed but are slightly further apart, governs vibration production. They suggest further that the descending neuron pIP10 affects the way sensory information modulate song choice (Calhoun, Pillow, and Murthy 2019). These findings point to an additional layer of signal control that is not only shaped by sensory cues but also internally in the male.

Finally, it is interesting to ask, at which level sensory cues and internal motor programs are integrated. We found that not only P1a activation was linked to a particular moving behavior of the male, but also pC2l activation. There was a trend of pC2l increasing velocity in solitary males during optogenetic stimulation (Figure 4G, even more pronounced in control flies of Figure 5B) and furthermore pC2l significantly decreased velocities at stimulus offset (when vibration co-occurred, Figure 4G). Notably, this effect disappeared as soon as the male was introduced to a female (Figure 6D). Similarly, male stopping behavior triggered by P1a activation disappeared in the presence of a female (Figure 7D). This suggests that female cues effect descending neurons or premotor circuits downstream of motor modulation by pC2l and P1a.

Summarizing, the way a communication signal is selected depends on context. Context-appropriate signal selection is guided by external cues and internal states. Sensory input from the visual system plausibly informs a male about which signal to select at a given moment. On top of that, internal, behavioral states shape signal selection. Male immobility is probably not only a part of the vibration motor program but also gating vibration output from the brain. This nicely illustrates the tight link of neurally controlled actions and the feedback-loop of exhibited behavior on neural output.

4.4 THE CIRCUIT UNDERLYING *DROSOPHILA* SONG AND VIBRATION CONTROL

We found two central neuron clusters to control song and vibration production: pC2l and P1a. Both of them drive the respective other signal type as well, suggesting a tight central integration of courtship signal control (Figure 4C,D). We propose a circuit model governing signal selection in the male brain (Figure 4B). In this model pC2l is upstream of a song descending neuron pIP10 but also of P1a, giving rise to the signal sequence of pulse, followed by vibrations upon pC2l activation (Figure 4C). P1a in turn is functionally upstream of a vibration descending neuron and a recurrent network, which together result in persistent vibrations upon P1a activation (Figure 4D). During pC2l or P1a activity we hardly observed output of the respective other signal type, which is why we postulate a mutual inhibition between the song and vibration output pathway. In our model both signal output descending neurons adapt with time, making the production of the other signal type possible after the activation phase.

Below are discussed, step by step, the evidence supporting our circuit model: starting from functional connectivity, to the dynamics responsible for signal output at stimulus offset and for persistence. We will discuss where the mutual inhibition could be implemented.

The next section addresses how female cues modulate the output of the circuit and discuss where cues act on the circuit. Finally, we will touch on the modulation of circuit dynamics by internal state and hypothesize what effect satiety has on the circuit.

4.4.1 *Evidence for our circuit model*

In our proposed model pC2l drives the song descending neuron pIP10 as well as P1a (Figure 4B). pC2l was recently shown to form direct synaptic contact with pIp10 (Lillvis et al.

2022). Furthermore, pC2l was suggested to be functionally upstream of pIP10 because both neurons drive a similar sequence of pulse and sine song at shorter stimulation durations but higher stimulation intensities than we use here (Roemschied et al. 2021). Besides driving pIP10, we postulate that pC2l is upstream of P1a as well. Such a connection was suggested previously by Roemschied et al. 2021 and our findings support this hypothesis. We find that pC2l at the offset of optogenetic stimulation drives vibrations (Figure 4C), which is probably mediated by P1a. One could test this by activating pC2l and simultaneously silencing P1a, the prediction would be that we loose the vibration offset in such an experiment. Similarly, stimulating pC2l while silencing pIP10 would probably diminish the song output observed for pC2l. Neural silencing is usually achieved by expressing the inward-rectifying potassium channels (Kir2.1, Baines et al. 2001). Another possibility is to block synaptic output by expressing tetanus toxin light chain (TNT, Sweeney et al. 1995) in the neurons of interest. However such an experiment requires previous genetic engineering of flies because in all neurons of interest – pC2l, P1a and pIP10 (Roemschied et al. 2021; Ding et al. 2019) – expression is achieved by a genetic intersection (Luan et al. 2006; Golic and Lindquist 1989).

Next, we propose that P1a is upstream of a descending neuron which drives vibrations. Descending neurons are usually the bottle neck of behavioral output and pass a behavioral command from the central brain to the ventral nerve cord (Namiki et al. 2018; Cande et al. 2018). It is likely that a descending neuron mediates the vibration output we observe upon P1a activation (Figure 4D). Using trans-synaptic tracing techniques such as *trans*-Tango (Talay et al. 2017) or an extensive examination of the male central brain connectome which will be available in the future (Scheffer et al. 2020) could aid finding such a descending neuron in case of direct synaptic contact. Another option is to screen though descending neurons which were shown before to induce immobility in flies (Cande et al. 2018) and find if they, upon optogenetic activation, drive vibration behavior.

The vibrations, as well as courtship song triggered by P1a activation outlasted the period of optogenetic stimulation (Figure 4D, more apparent in control flies of Figure 5C). Such persistent output is likely mediated by pCd, a cluster that recurrently connects to P1a, prolonging the output of social behavior such as aggression or wing extension mediated by P1a (Jung et al. 2020; Zhang, Rogulja, and Crickmore 2019; Zhang, Miner, et al. 2018). Again, a straight-forward way to test this hypothesis would be to optogenetically activate P1a while pCd neurons are silenced or have blocked synaptic output.

P1a activation drives not only vibrations but also song. In our model this link is depicted by a connection via the recurrent neuron pCd to pIP10. However, more accurately: the hypothesized connection between pCd and pIP10 is not sufficient to drive song but requires additional P1a activity (Jung et al. 2020). pIP10 was suggested to be downstream of P1 in the past (Philipsborn et al. 2011) and a functional link between them was recently confirmed by the finding that co-activation of pIP10 and P1a strongly boosts pIP10 song output (Roemschied et al. 2021).

Finally, we suggest in our circuit model that the pathways for signal type output inhibit each other. During pC2l activation we only observe pulse production, a little sine but no vibration production (Figure 4C). Vice versa, during P1a activation the males vibrate but

hardly sing (Figure 4D). This mutual inhibition becomes very apparent when introducing the males to a female and stimulating either neuron. For the time of optogenetic stimulation of pC2l the output of vibrations is significantly reduced (Figure 6B) and in contrast during P1a stimulation the males hardly sing (Figure 7B). In our circuit scheme the mutual inhibition is schematically depicted between the vibration and song descending neuron (Figure 4B), however such a cross-inhibition could realistically be implemented in the central brain or the ventral nerve cord by inhibitory interneurons. Such interneurons could act on descending neurons or their downstream targets: pattern generators and motor neurons. A circuit motif, involving mutual inhibition and rebound excitability was postulated before to enable complex song generation of pulse and sine song in the ventral nerve cord (Roemschied et al. 2021). Opposingly, a direct inhibitory connection from P1a to the song pathway is implausible. Findings that co-activation of pIP10 and P1a strongly enhances song output (Roemschied et al. 2021) and that P1a activation in other studies drives wing extensions or singing in males (Hoopfer et al. 2015; Jung et al. 2020; Clemens et al. 2018) disagree with the idea of P1a inhibiting song output.

It would be interesting to study the time scales and tuning of signal control by P1a and pC2l in more detail. Varying the duration or intensity of their optogenetic activation could for example reveal if the signal type output of P1a is dose-dependent. Brief P1a activation could be insufficient for P1a to drive persistent signal output whereas stronger P1a stimulation could result in higher song output probabilities. This would underline the role of P1a in gating courtship arousal (Hindmarsh Sten et al. 2021) and presumably link the different signals (song and vibration) to distinct arousal intensities. Such results would be in line with previous findings that P1a promotes aggression at a lower activation threshold than required for wing extension (Hoopfer et al. 2015). Similarly, brief or weak pC2l stimulation could be insufficient to co-active P1a in our circuit and reduce the vibration offset response. In contrast, stronger or longer pC2l activation would also increase P1a activity and could even be sufficient for pCd to kick in and drive persistent vibrations or song after the stimulation period.

To sum up, a combination of anatomical and functional studies support the connectivity we propose in our circuit. Testing this circuit further by simultaneous activation and inhibition of different neural nodes in the circuit could confirm the identities of suggested neurons (pIP10 and pCd). It is still unclear at which level the mutual inhibition between signal output is implemented. And more detailed analyses of dose-dependent signal control of P1a and pC2l would not only uncover the scope of their functional connectivity but also support to unravel the versatile roles of P1a in regulating social behavior.

4.4.2 *Circuit modulation by cues and state*

After finding that pC2l and P1a control courtship signal production in males with complex dynamics, we tested how a change in internal state or exposure to social cues would affect these dynamics.

We changed the males' courtship drive by sexually satiating them (Figure 5A). A reduced

courtship drive abolished the vibration offset after pC2l activation (Figure 5B) as well as the vibration persistence upon P1a activation (Figure 5C).

Sexual drive presumably acts on two of our circuit nodes: P1a and pCd. P1 neurons in sexually motivated males were shown to be less sensitive to inhibition (Zhang, Rogulja, and Crickmore 2019; Zhang, Miner, et al. 2018) and recurrent circuits such as pCd (but also NPF, Zhang, Rogulja, and Crickmore 2019) are more excitable in motivated males. pCd was shown to induce an internal state of social arousal lasting for several minutes (Jung et al. 2020) and is a good candidate mediating the persistent vibrations upon P1a stimulation that we observe. Reduced excitability of pCd in satiated males could be therefore the mechanism by which the vibration persistence abolishes. However, pCd only amplifies behaviors but requires P1a to initially induce behavioral output. With this in mind, a reduced excitability of P1a in satiated males may not be sufficient to drive pCd in the first place, suggesting that the effect of satiety on P1a could be sufficient to abolish long lasting vibration output. The reduced excitability of P1a is furthermore a plausible mechanism why we loose the vibration offset when activating pC2l in satiated males. The idea is that, even though pC2l is active, P1a activity does not reach a threshold which would yield vibration output. If satiety affects pC2l excitability as well requires further investigation.

Our next step was to examine how female cues modulate the output of the courtship signal circuit. For this, we exposed each male to a female and respectively activated pC2l and P1a in the male (Figures 6A and 7A). We found that our circuit was neither agnostic to the social cues nor that the social cues completely overwrote the circuit outputs. Instead, circuit output directly mediated during the activity of our circuit nodes pC2l and P1a were agnostic to cues whereas downstream effects were quickly modulated by female cues.

One direct effect observed during pC2l and P1a activity was the mutual inhibition between the output of both signal types (song and vibration). This cross-inhibition became very apparent when the males were courting a female. During pC2l activity, vibration output was strongly reduced (Figure 6B) and during P1a stimulation, the males hardly sang (Figure 7B). The second direct effect of pC2l was to drive song output and of P1a to drive vibration output. In the presence of female cues, pC2l still strongly drove pulse song (Figure 6B) and P1a still yielded vibration output. But the vibration output of P1a was not significantly different to vibration generation of the male after stimulation (Figure 7B). Hence, in the case of signal output, social cues seem to affect pC2l and P1a differently. Song production mediated by pC2l is agnostic to female cues. Vibration production, however, is a slightly different case. First of all, we find that vibration production is mediated by P1a. Though P1a does not only drive vibrations but also other social behaviors, such as wing extension, song and even aggressive behaviors (Hoopfer et al. 2015; Jung et al. 2020; Clemens et al. 2018) depending on intensity of activation or activation tool. Accordingly, vibration output is just one role out of the complex functions which P1a fulfills in social behavior. It is therefore plausible that P1a undergoes stronger cue modulation than pC2l, to allow for the appropriate behavioral output. Secondly, males can sing regardless of their walking behavior, vibrations on the other hand coincide with

male immobility. Therefore vibration output is likely gated by male motor state (as discussed above, Subsection 4.3.2). Generalizing, we suggest that circuit dynamics during the time of pC2l or P1a activity, namely the mutual inhibition motif and the preference for a particular signal output, are agnostic to social cues.

Let us have a look at the downstream effects of the circuits' dynamics. In case of pC2l we observed vibration generation which followed the offset of optogenetic stimulation whereas in case of P1a males preferentially continued to vibrate after stimulation offset (Figures 6B and 7B). Both of these effects are overwritten by social cues: quickly after stimulation offset all males sang or vibrated at baseline level (Figures 6B and 7B). The only striking effect which be observe after optogenetic stimulation stopped is that males briefly close their wings after pC2l was active (Figure 6E). We reason that this wing closure is indicative for short P1a activity, because P1a activation in presence of a female results in male wing closure, too (Figure 7E).

Taken together, our results suggest that when exposed to female cues, both circuit nodes pC2l and P1a reinforce the exclusiveness of either signal output when active. While P1a still allows for vibration output depending on male motor state, pC2l actively drives pulse production regardless of sensory input. Finally, the more complex dynamics which we observe in solitary males result from functional connectivity and physiological properties of the nodes within the circuit. But these complex dynamics are highly adaptable to social input as well as internal states such as high or low courtship drive. A tight central integration for the control of communication signals probably evolved because is allows for context-dependent signal selection and flexible signal switching. Our findings bring together the notion of a circuit motif with a pre-wired, effective connectivity and its flexible adaptation to contexts and tasks.

4.5 CONCLUSION

With this thesis we shed light on social communication and its underlying neural mechanisms. We use the model system *Drosophila melanogaster* with its elaborate courtship ritual to study the context, circuit and modulation of signal selection. Our quantitative approach enabled us to define in which situation a male chooses for one signal type rather than for another. With optogenetic experiments we identified neurons controlling the different signal types with complex dynamics and inferred an underlying circuit. By probing this circuit in different naturalistic settings, we showed that the circuits output is modulated by internal courtship drive as well as external social cues. Together these findings demonstrate that both, internal state and social cues, interact with intrinsic circuit dynamics to drive the selection between two communication signals.

BIBLIOGRAPHY

Agrawal, S., Dickinson, E.S., Sustar, A., Gurung, P., Shepherd, D., Truman, J.W., and Tuthill, J.C. (2020). Central processing of leg proprioception in Drosophila. eLife *9*. R.L. Calabrese, E. Marder, and T. Fujiwara, ed., e60299.

Anderson, D.J. (2016). Circuit modules linking internal states and social behaviour in flies and mice. Nature Reviews Neuroscience *17*.11, 692–704.

Angstadt, J.D., Grassmann, J.L., Theriault, K.M., and Levasseur, S.M. (2005). Mechanisms of postinhibitory rebound and its modulation by serotonin in excitatory swim motor neurons of the medicinal leech. Journal of Comparative Physiology A *191*.8, 715–732.

Arthur, B.J., Sunayama-Morita, T., Coen, P., Murthy, M., and Stern, D.L. (2013). Multi-channel acoustic recording and automated analysis of Drosophila courtship songs. BMC Biology *11*.1, 11.

Baines, R.A., Uhler, J.P., Thompson, A., Sweeney, S.T., and Bate, M. (2001). Altered Electrical Properties in DrosophilaNeurons Developing without Synaptic Transmission. Journal of Neuroscience *21*.5, 1523–1531.

Baker, C.A., McKellar, C., Pang, R., Nern, A., Dorkenwald, S., Pacheco, D.A., Eckstein, N., Funke, J., Dickson, B.J., and Murthy, M. (2022). Neural network organization for courtship-song feature detection in Drosophila. Current Biology *32*.15, 3317–3333.e7.

Baker, C.A., Clemens, J., and Murthy, M. (2019). Acoustic Pattern Recognition and Courtship Songs: Insights from Insects. Annual review of neuroscience *42*, 129–147.

Battaglia, D., Witt, A., Wolf, F., and Geisel, T. (2012). Dynamic Effective Connectivity of Inter-Areal Brain Circuits. PLOS Computational Biology *8*.3, e1002438.

Bennet-Clark, H.C. and Ewing, A.W. (1969). Pulse interval as a critical parameter in the courtship song of Drosophila melanogaster. Animal Behaviour *17*.4, 755–759.

Bidaye, S.S., Laturney, M., Chang, A.K., Liu, Y., Bockemühl, T., Büschges, A., and Scott, K. (2020). Two Brain Pathways Initiate Distinct Forward Walking Programs in Drosophila. Neuron *108*.3, 469–485.e8.

Bolhuis, J.J., Okanoya, K., and Scharff, C. (2010). Twitter evolution: converging mechanisms in birdsong and human speech. Nature Reviews Neuroscience *11*.11, 747–759.

Bradbury, J.W. and Vehrencamp, S.L. (2011). Principles of Animal Communication 2nd ed. ().

Brand, A. and Perrimon, N. (1993). Targeted gene expression as a means of altering cell fates and generating dominant phenotypes. Development *118*.2, 401–415.

Brieger, G. and Butterworth, F.M. (1970). Drosophila melanogaster: Identity of Male Lipid in Reproductive System. Science *167*.3922, 1262–1262.

Broder, E.D., Wikle, A.W., Gallagher, J.H., and Tinghitella, R.M. (2021). Substrate-borne vibration in Pacific field cricket courtship displays. Journal of Orthoptera Research *30*.1, 43–50.

Bussell, J.J., Yapici, N., Zhang, S.X., Dickson, B.J., and Vosshall, L.B. (2014). Abdominal-B Neurons Control Drosophila Virgin Female Receptivity. Current Biology *24*.14, 1584–1595.

Cachero, S., Gkantia, M., Bates, A.S., Frechter, S., Blackie, L., McCarthy, A., Sutcliffe, B., Strano, A., Aso, Y., and Jefferis, G.S.X.E. (2020). BAcTrace, a tool for retrograde tracing of neuronal circuits in Drosophila. Nature Methods *17*.12, 1254–1261.

Cachero, S., Ostrovsky, A.D., Yu, J.Y., Dickson, B.J., and Jefferis, G.S.X.E. (2010). Sexual Dimorphism in the Fly Brain. Current Biology *20*.18, 1589–1601.

Calhoun, A.J., Pillow, J.W., and Murthy, M. (2019). Unsupervised identification of the internal states that shape natural behavior. Nature Neuroscience *22*.12, 2040–2049.

Cande, J., Namiki, S., Qiu, J., Korff, W., Card, G.M., Shaevitz, J.W., Stern, D.L., and Berman, G.J. (2018). Optogenetic dissection of descending behavioral control in Drosophila. eLife *7*. K. Scott, ed., e34275.

Chen, C.-L., Aymanns, F., Minegishi, R., Matsuda, V.D.V., Talabot, N., Günel, S., Dickson, B.J., and Ramdya, P. (2022). *Ascending neurons convey behavioral state to integrative sensory and action selection centers in the brain*. URL: https://www.biorxiv.org/content/10.1101/2022.02.09.479566v1 (visited on 12/01/2022).

Chen, D., Sitaraman, D., Chen, N., Jin, X., Han, C., Chen, J., Sun, M., Baker, B.S., Nitabach, M.N., and Pan, Y. (2017). Genetic and neuronal mechanisms governing the sex-specific interaction between sleep and sexual behaviors in Drosophila. Nature Communications *8*.1, 154.

Cheriyamkunnel, S.J., Rose, S., Jacob, P.F., Blackburn, L.A., Glasgow, S., Moorse, J., Winstanley, M., Moynihan, P.J., Waddell, S., and Rezaval, C. (2021). A neuronal mechanism controlling the choice between feeding and sexual behaviors in Drosophila. Current Biology *31*.19, 4231–4245.e4.

Clemens, J., Coen, P., Roemschied, F.A., Pereira, T.D., Mazumder, D., Aldarondo, D.E., Pacheco, D.A., and Murthy, M. (2018). Discovery of a New Song Mode in Drosophila Reveals Hidden Structure in the Sensory and Neural Drivers of Behavior. Current Biology *28*.15, 2400–2412.e6.

Clowney, E.J., Iguchi, S., Bussell, J.J., Scheer, E., and Ruta, V. (2015). Multimodal Chemosensory Circuits Controlling Male Courtship in Drosophila. Neuron *87*.5, 1036–1049.

Clyne, J.D. and Miesenböck, G. (2008). Sex-Specific Control and Tuning of the Pattern Generator for Courtship Song in Drosophila. Cell *133*.2, 354–363.

Cocroft, R.B. and Rodríguez, R.L. (2005). The Behavioral Ecology of Insect Vibrational Communication. BioScience *55*.4, 323–334.

Coen, P., Clemens, J., Weinstein, A.J., Pacheco, D.A., Deng, Y., and Murthy, M. (2014). Dynamic sensory cues shape song structure in Drosophila. Nature *507*.7491, 233–237.

Coffey, K.R., Marx, R.G., and Neumaier, J.F. (2019). DeepSqueak: a deep learning-based system for detection and analysis of ultrasonic vocalizations. Neuropsychopharmacology *44*.5, 859–868.

Cohen, Y., Nicholson, D.A., Sanchioni, A., Mallaber, E.K., Skidanova, V., and Gardner, T.J. (2022). Automated annotation of birdsong with a neural network that segments spectrograms. eLife *11*. J.H. Goldberg, R.L. Calabrese, J.H. Goldberg, and M. Brainard, ed., e63853.

Deutsch, D., Clemens, J., Thiberge, S.Y., Guan, G., and Murthy, M. (2019). Shared Song Detector Neurons in Drosophila Male and Female Brains Drive Sex-Specific Behaviors. Current Biology *29*.19, 3200–3215.e5.

Devineni, A.V. and Scaplen, K.M. (2022). Neural Circuits Underlying Behavioral Flexibility: Insights From Drosophila. Frontiers in Behavioral Neuroscience *15*.

Ding, Y., Lillvis, J.L., Cande, J., Berman, G.J., Arthur, B.J., Long, X., Xu, M., Dickson, B.J., and Stern, D.L. (2019). Neural Evolution of Context-Dependent Fly Song. Current Biology *29*.7, 1089–1099.e7.

Duckhorn, J.C., Cande, J., Metkus, M.C., Song, H., Altamirano, S., Stern, D.L., and Shirangi, T.R. (2022). Regulation of Drosophila courtship behavior by the Tlx/tailless-like nuclear receptor, dissatisfaction. Current Biology *32*.8, 1703–1714.e3.

Dukas, R. (2020). Natural history of social and sexual behavior in fruit flies. Scientific Reports *10*.1, 21932.

Ejima, A. and Griffith, L.C. (2008). Courtship Initiation Is Stimulated by Acoustic Signals in Drosophila melanogaster. PLOS ONE *3*.9, e3246.

Ewing, A.W. (1978). The antenna of Drosophila as a 'love song' receptor. Physiological Entomology *3*.1, 33–36.

Fabre, C.C.G., Hedwig, B., Conduit, G., Lawrence, P.A., Goodwin, S.F., and Casal, J. (2012). Substrate-Borne Vibratory Communication during Courtship in Drosophila melanogaster. Current Biology *22*.22, 2180–2185.

Field, L.H. and Matheson, T. (1998). "Chordotonal Organs of Insects." Advances in Insect Physiology, P.D. Evans, ed. Vol. 27. (Academic Press), pp. 1–228.

Flavell, S.W., Gogolla, N., Lovett-Barron, M., and Zelikowsky, M. (2022). The emergence and influence of internal states. Neuron *110*.16, 2545–2570.

Golic, K.G. and Lindquist, S. (1989). The FLP recombinase of yeast catalyzes site-specific recombination in the drosophila genome. Cell *59*.3, 499–509.

Göpfert, M.C. and Robert, D. (2002). The mechanical basis of Drosophila audition. Journal of Experimental Biology *205*.9, 1199–1208.

Gorter, J.A., Jagadeesh, S., Gahr, C., Boonekamp, J.J., Levine, J.D., and Billeter, J.-C. (2016). The nutritional and hedonic value of food modulate sexual receptivity in Drosophila melanogaster females. Scientific Reports *6*.1, 19441.

Graving, J.M., Chae, D., Naik, H., Li, L., Koger, B., Costelloe, B.R., and Couzin, I.D. (2019). DeepPoseKit, a software toolkit for fast and robust animal pose estimation using deep learning. eLife *8*. I.T. Baldwin, J.W. Shaevitz, J.W. Shaevitz, and G. Stephens, ed., e47994.

Hahnloser, R.H.R., Kozhevnikov, A.A., and Fee, M.S. (2002). An ultra-sparse code underliesthe generation of neural sequences in a songbird. Nature *419*.6902, 65–70.

Hernández, M.V. and Fabre, C.C.G. (2016). The Elaborate Postural Display of Courting Drosophila persimilis Flies Produces Substrate-Borne Vibratory Signals. Journal of Insect Behavior *29*.5, 578–590.

Hill, P.S.M. (2001). Vibration and Animal Communication: A Review1. American Zoologist *41*.5, 1135–1142.

Hindmarsh Sten, T., Li, R., Otopalik, A., and Ruta, V. (2021). Sexual arousal gates visual processing during Drosophila courtship. Nature *595*.7868, 549–553.

Hoopfer, E.D., Jung, Y., Inagaki, H.K., Rubin, G.M., and Anderson, D.J. (2015). P1 interneurons promote a persistent internal state that enhances inter-male aggression in Drosophila. eLife *4*. M. Ramaswami, ed., e11346.

Inagaki, H.K., Jung, Y., Hoopfer, E.D., Wong, A.M., Mishra, N., Lin, J.Y., Tsien, R.Y., and Anderson, D.J. (2014). Optogenetic control of Drosophila using a red-shifted channelrhodopsin reveals experience-dependent influences on courtship. Nature Methods *11*.3, 325–332.

Jiang, X. and Pan, Y. (2022). Neural Control of Action Selection Among Innate Behaviors. Neuroscience Bulletin *38*.12, 1541–1558.

Jung, Y., Kennedy, A., Chiu, H., Mohammad, F., Claridge-Chang, A., and Anderson, D.J. (2020). Neurons that Function within an Integrator to Promote a Persistent Behavioral State in Drosophila. Neuron *105*.2, 322–333.e5.

Jürgens, U. (1994). The role of the periaqueductal grey in vocal behaviour. Behavioural Brain Research *62*.2, 107–117.

Kallman, B.R., Kim, H., and Scott, K. (2015). Excitation and inhibition onto central courtship neurons biases Drosophila mate choice. eLife *4*. M. Ramaswami, ed., e11188.

Kamikouchi, A., Shimada, T., and Ito, K. (2006). Comprehensive classification of the auditory sensory projections in the brain of the fruit fly Drosophila melanogaster. Journal of Comparative Neurology *499*.3, 317–356.

Kim, J. et al. (2003). A TRPV family ion channel required for hearing in Drosophila. Nature *424*.6944, 81–84.

Kimura, K.-i., Sato, C., Koganezawa, M., and Yamamoto, D. (2015). Drosophila Ovipositor Extension in Mating Behavior and Egg Deposition Involves Distinct Sets of Brain Interneurons. PLOS ONE *10*.5, e0126445.

Klapoetke, N.C. et al. (2014). Independent optical excitation of distinct neural populations. Nature Methods *11*.3, 338–346.

Kohatsu, S., Koganezawa, M., and Yamamoto, D. (2011). Female Contact Activates Male-Specific Interneurons that Trigger Stereotypic Courtship Behavior in Drosophila. Neuron *69*.3, 498–508.

Kohatsu, S. and Yamamoto, D. (2015). Visually induced initiation of Drosophila innate courtship-like following pursuit is mediated by central excitatory state. Nature Communications *6*.1, 6457.

Kuan, A.T. et al. (2022). *Synaptic wiring motifs in posterior parietal cortex support decision-making*. URL: https://www.biorxiv.org/content/10.1101/2022.04.13.488176v1 (visited on 12/01/2022).

Kupfermann, I. and Weiss, K.R. (2001). Motor program selection in simple model systems. Current Opinion in Neurobiology *11*.6, 673–677.

Kurtovic, A., Widmer, A., and Dickson, B.J. (2007). A single class of olfactory neurons mediates behavioural responses to a Drosophila sex pheromone. Nature *446*.7135, 542–546.

Larsson, M.C., Domingos, A.I., Jones, W.D., Chiappe, M.E., Amrein, H., and Vosshall, L.B. (2004). Or83b Encodes a Broadly Expressed Odorant Receptor Essential for Drosophila Olfaction. Neuron *43*.5, 703–714.

Lasbleiz, C., Ferveur, J.-F., and Everaerts, C. (2006). Courtship behaviour of Drosophila melanogaster revisited. Animal Behaviour *72*.5, 1001–1012.

Li, X., Ishimoto, H., and Kamikouchi, A. (2018). Auditory experience controls the maturation of song discrimination and sexual response in Drosophila. eLife *7*. L.C. Griffith, ed., e34348.

Lillvis, J.L. et al. (2022). Rapid reconstruction of neural circuits using tissue expansion and light sheet microscopy. eLife *11*. M. Louis and C. Desplan, ed., e81248.

Long, M.A., Jin, D.Z., and Fee, M.S. (2010). Support for a synaptic chain model of neuronal sequence generation. Nature *468*.7322, 394–399.

Luan, H., Peabody, N.C., Vinson, C.R., and White, B.H. (2006). Refined Spatial Manipulation of Neuronal Function by Combinatorial Restriction of Transgene Expression. Neuron *52*.3, 425–436.

Machado, D.R., Afonso, D.J., Kenny, A.R., Öztürk-Çolak, A., Moscato, E.H., Mainwaring, B., Kayser, M., and Koh, K. (2017). Identification of octopaminergic neurons that modulate sleep suppression by male sex drive. eLife *6*. L.C. Griffith, ed., e23130.

Machens, C.K., Romo, R., and Brody, C.D. (2005). Flexible Control of Mutual Inhibition: A Neural Model of Two-Interval Discrimination. Science *307*.5712, 1121–1124.

Mamiya, A., Gurung, P., and Tuthill, J.C. (2018). Neural Coding of Leg Proprioception in Drosophila. Neuron *100*.3, 636–650.e6.

Marder, E. and Calabrese, R.L. (1996). Principles of rhythmic motor pattern generation. Physiological Reviews *76*.3, 687–717.

Markow, T.A. and Hanson, S.J. (1981). Multivariate analysis of Drosophila courtship. Proceedings of the National Academy of Sciences *78*.1, 430–434.

Mathis, A., Mamidanna, P., Cury, K.M., Abe, T., Murthy, V.N., Mathis, M.W., and Bethge, M. (2018). DeepLabCut: markerless pose estimation of user-defined body parts with deep learning. Nature Neuroscience *21*.9, 1281–1289.

Mauss, A.S., Busch, C., and Borst, A. (2017). Optogenetic Neuronal Silencing in Drosophila during Visual Processing. Scientific Reports *7*.1, 13823.

Mayr, E. (1961). Cause and Effect in Biology. Science *134*.3489, 1501–1506.

Mazzoni, V., Anfora, G., and Virant-Doberlet, M. (2013). Substrate Vibrations during Courtship in Three Drosophila species. PLOS ONE *8*.11, e80708.

McKellar, C.E., Lillvis, J.L., Bath, D.E., Fitzgerald, J.E., Cannon, J.G., Simpson, J.H., and Dickson, B.J. (2019). Threshold-Based Ordering of Sequential Actions during Drosophila Courtship. Current Biology *29*.3, 426–434.e6.

McKelvey, E.G.Z., Gyles, J.P., Michie, K., Pancorbo, V.B., Sober, L., Kruszewski, L.E., Chan, A., and Fabre, C.C.G. (2021). Drosophila females receive male substrate-borne signals through specific leg neurons during courtship. Current Biology *31*.17, 3894–3904.e5.

McKinney, R.M. and Ben-Shahar, Y. (2019). *Visual recognition of the female body axis drives spatial elements of male courtship in Drosophila melanogaster*. URL: https://www.biorxiv.org/content/10.1101/576322v1 (visited on 12/17/2022).

Mendes, C.S., Bartos, I., Akay, T., Márka, S., and Mann, R.S. (2013). Quantification of gait parameters in freely walking wild type and sensory deprived Drosophila melanogaster. eLife *2*. R. Calabrese, ed., e00231.

Mezzera, C., Brotas, M., Gaspar, M., Pavlou, H.J., Goodwin, S.F., and Vasconcelos, M.L. (2020). Ovipositor Extrusion Promotes the Transition from Courtship to Copulation and Signals Female Acceptance in Drosophila melanogaster. Current Biology *30*.19, 3736–3748.e5.

Mooney, R. (2000). Different Subthreshold Mechanisms Underlie Song Selectivity in Identified HVc Neurons of the Zebra Finch. Journal of Neuroscience *20*.14, 5420–5436.

Mooney, R. and Prather, J.F. (2005). The HVC Microcircuit: The Synaptic Basis for Interactions between Song Motor and Vocal Plasticity Pathways. Journal of Neuroscience *25*.8, 1952–1964.

Morris, G. and Luca, P.d. (1998). Courtship Communication in Meadow Katydids: Female Preference for Large Male Vibrations. Behaviour *135*.6, 777–794.

Musall, S., Kaufman, M.T., Juavinett, A.L., Gluf, S., and Churchland, A.K. (2019). Single-trial neural dynamics are dominated by richly varied movements. Nature Neuroscience *22*.10, 1677–1686.

Namiki, S., Dickinson, M.H., Wong, A.M., Korff, W., and Card, G.M. (2018). The functional organization of descending sensory-motor pathways in Drosophila. eLife *7*. K. Scott, ed., e34272.

O'Sullivan, A., Lindsay, T., Prudnikova, A., Erdi, B., Dickinson, M., and Philipsborn, A.C.v. (2018). Multifunctional Wing Motor Control of Song and Flight. Current Biology *28*.17, 2705–2717.e4.

Pacheco, D.A., Thiberge, S.Y., Pnevmatikakis, E., and Murthy, M. (2021). Auditory activity is diverse and widespread throughout the central brain of Drosophila. Nature Neuroscience *24*.1, 93–104.

Patella, P. and Wilson, R.I. (2018). Functional Maps of Mechanosensory Features in the Drosophila Brain. Current Biology *28*.8, 1189–1203.e5.

Pedregosa, F. et al. (2011). Scikit-learn: Machine Learning in Python. The Journal of Machine Learning Research *12* (null), 2825–2830.

Pereira, T.D., Aldarondo, D.E., Willmore, L., Kislin, M., Wang, S.S.-H., Murthy, M., and Shaevitz, J.W. (2019). Fast animal pose estimation using deep neural networks. Nature Methods *16*.1, 117–125.

Phelps, J.S. et al. (2021). Reconstruction of motor control circuits in adult Drosophila using automated transmission electron microscopy. Cell *184*.3, 759–774.e18.

Philipsborn, A.C.v., Liu, T., Yu, J.Y., Masser, C., Bidaye, S.S., and Dickson, B.J. (2011). Neuronal Control of Drosophila Courtship Song. Neuron *69*.3, 509–522.

Prescott, T.J. (2008). Action selection. Scholarpedia *3*.2, 2705.

Ramdya, P., Lichocki, P., Cruchet, S., Frisch, L., Tse, W., Floreano, D., and Benton, R. (2015). Mechanosensory interactions drive collective behaviour in Drosophila. Nature *519*.7542, 233–236.

Ribeiro, I.M.A., Drews, M., Bahl, A., Machacek, C., Borst, A., and Dickson, B.J. (2018). Visual Projection Neurons Mediating Directed Courtship in Drosophila. Cell *174*.3, 607–621.e18.

Roach, J.P., Churchland, A.K., and Engel, T.A. (2022). *Two roles for choice selective inhibition in decision-making circuits*. URL: https://www.biorxiv.org/content/10.1101/2022.01.24.477635v1 (visited on 12/01/2022).

Roemschied, F.A., Pacheco, D.A., Ireland, E.C., Li, X., Aragon, M.J., Pang, R., and Murthy, M. (2021). *Flexible Circuit Mechanisms for Context-Dependent Song Sequencing*. URL: https://www.biorxiv.org/content/10.1101/2021.11.01.466727v1 (visited on 12/01/2022).

Rybak, F., Aubin, T., Moulin, B., and Jallon, J.-M. (2002). Acoustic communication in Drosophila melanogaster courtship: Are pulse- and sine-song frequencies important for courtship success? Canadian Journal of Zoology *80*.6, 987–996.

Scheffer, L.K. et al. (2020). A connectome and analysis of the adult Drosophila central brain. eLife *9*. E. Marder, M.B. Eisen, J. Pipkin, and C.Q. Doe, ed., e57443.

Seeds, A.M., Ravbar, P., Chung, P., Hampel, S., Midgley Jr, F.M., Mensh, B.D., and Simpson, J.H. (2014). A suppression hierarchy among competing motor programs drives sequential grooming in Drosophila. eLife *3*. R.L. Calabrese, ed., e02951.

Seeholzer, L.F., Seppo, M., Stern, D.L., and Ruta, V. (2018). Evolution of a central neural circuit underlies Drosophila mate preferences. Nature *559*.7715, 564–569.

Setoguchi, S., Takamori, H., Aotsuka, T., Sese, J., Ishikawa, Y., and Matsuo, T. (2014). Sexual dimorphism and courtship behavior in Drosophila prolongata. Journal of Ethology *32*.2, 91–102.

Shirangi, T.R., Wong, A.M., Truman, J.W., and Stern, D.L. (2016). Doublesex Regulates the Connectivity of a Neural Circuit Controlling Drosophila Male Courtship Song. Developmental Cell *37*.6, 533–544.

Shorey, H.H. (1962). Nature of the Sound Produced by Drosophila melanogaster during Courtship. Science *137*.3531, 677–678.

Solis, M.M. and Perkel, D.J. (2005). Rhythmic Activity in a Forebrain Vocal Control Nucleus In Vitro. Journal of Neuroscience *25*.11, 2811–2822.

Sorkaç, A., Moșneanu, R.A., Crown, A.M., Savaş, D., Okoro, A.M., Talay, M., and Barnea, G. (2022). *retro-Tango enables versatile retrograde circuit tracing in Drosophila*. URL: https://www.biorxiv.org/content/10.1101/2022.11.24.517859v1 (visited on 12/18/2022).

Steinfath, E., Palacios-Muñoz, A., Rottschäfer, J.R., Yuezak, D., and Clemens, J. (2021). Fast and accurate annotation of acoustic signals with deep neural networks. eLife *10*. R.L. Calabrese, S.R. Egnor, and T. Troyer, ed., e68837.

Stritih-Peljhan, N. and Virant-Doberlet, M. (2021). Vibrational signalling, an underappreciated mode in cricket communication. The Science of Nature *108*.5, 41.

Strother, J.A., Wu, S.-T., Wong, A.M., Nern, A., Rogers, E.M., Le, J.Q., Rubin, G.M., and Reiser, M.B. (2017). The Emergence of Directional Selectivity in the Visual Motion Pathway of Drosophila. Neuron *94*.1, 168–182.e10.

Swain, B. and Philipsborn, A.C.v. (2021). "Chapter Three - Sound production in Drosophila melanogaster: Behaviour and neurobiology." Advances in Insect Physiology, R. Jurenka, ed. Vol. 61. Sound Communication in Insects. (Academic Press), pp. 141–187.

Sweeney, S.T., Broadie, K., Keane, J., Niemann, H., and O'Kane, C.J. (1995). Targeted expression of tetanus toxin light chain in Drosophila specifically eliminates synaptic transmission and causes behavioral defects. Neuron *14*.2, 341–351.

Taisz, I. et al. (2022). *Generating parallel representations of position and identity in the olfactory system*. URL: https://www.biorxiv.org/content/10.1101/2022.05.13.491877v1 (visited on 12/17/2022).

Talay, M. et al. (2017). Transsynaptic Mapping of Second-Order Taste Neurons in Flies by trans-Tango. Neuron *96*.4, 783–795.e4.

Tschida, K., Michael, V., Takatoh, J., Han, B.-X., Zhao, S., Sakurai, K., Mooney, R., and Wang, F. (2019). A Specialized Neural Circuit Gates Social Vocalizations in the Mouse. Neuron *103*.3, 459–472.e4.

Tsubouchi, A., Yano, T., Yokoyama, T.K., Murtin, C., Otsuna, H., and Ito, K. (2017). Topological and modality-specific representation of somatosensory information in the fly brain. Science *358*.6363, 615–623.

Tsuyama, T., Kishikawa, J.-i., Han, Y.-W., Harada, Y., Tsubouchi, A., Noji, H., Kakizuka, A., Yokoyama, K., Uemura, T., and Imamura, H. (2013). In Vivo Fluorescent Adenosine 5′-Triphosphate (ATP) Imaging of Drosophila melanogaster and Caenorhabditis elegans by Using a Genetically Encoded Fluorescent ATP Biosensor Optimized for Low Temperatures. Analytical Chemistry *85*.16, 7889–7896.

Voorhies, W.A.V. (2009). Metabolic function in Drosophila melanogaster in response to hypoxia and pure oxygen. Journal of Experimental Biology *212*.19, 3132–3141.

Wang, K., Wang, F., Forknall, N., Yang, T., Patrick, C., Parekh, R., and Dickson, B.J. (2021). Neural circuit mechanisms of sexual receptivity in Drosophila females. Nature *589*.7843, 577–581.

Wang, X.-J. (2008). Decision Making in Recurrent Neuronal Circuits. Neuron *60*.2, 215–234.

Weber, A.I. and Pillow, J.W. (2017). Capturing the Dynamical Repertoire of Single Neurons with Generalized Linear Models. Neural Computation *29*.12, 3260–3289.

Weidemann, S. and Keuper, A. (1987). Influence of vibratory signals on the phonotaxis of the gryllid Gryllus bimaculatus DeGeer (Ensifera: Gryllidae). Oecologia *74*.2, 316–318.

Yamada, D., Ishimoto, H., Li, X., Kohashi, T., Ishikawa, Y., and Kamikouchi, A. (2018). GABAergic Local Interneurons Shape Female Fruit Fly Response to Mating Songs. Journal of Neuroscience *38*.18, 4329–4347.

Yamamoto, D. and Koganezawa, M. (2013). Genes and circuits of courtship behaviour in Drosophila males. Nature Reviews Neuroscience *14*.10, 681–692.

Yeh, S.-D., Liou, S.-R., and True, J.R. (2006). Genetics of divergence in male wing pigmentation and courtship behavior between Drosophila elegans and D. gunungcola. Heredity *96*.5, 383–395.

Yoon, J., Matsuo, E., Yamada, D., Mizuno, H., Morimoto, T., Miyakawa, H., Kinoshita, S., Ishimoto, H., and Kamikouchi, A. (2013). Selectivity and Plasticity in a Sound-Evoked Male-Male Interaction in Drosophila. PLOS ONE *8*.9, e74289.

Yu, J.Y., Kanai, M.I., Demir, E., Jefferis, G.S.X.E., and Dickson, B.J. (2010). Cellular Organization of the Neural Circuit that Drives Drosophila Courtship Behavior. Current Biology *20*.18, 1602–1614.

Zhang, S.X., Miner, L.E., Boutros, C.L., Rogulja, D., and Crickmore, M.A. (2018). Motivation, Perception, and Chance Converge to Make a Binary Decision. Neuron *99*.2, 376–388.e6.

Zhang, S.X., Rogulja, D., and Crickmore, M.A. (2016). Dopaminergic Circuitry Underlying Mating Drive. Neuron *91*.1, 168–181.

Zhang, S.X., Rogulja, D., and Crickmore, M.A. (2019). Recurrent Circuitry Sustains Drosophila Courtship Drive While Priming Itself for Satiety. Current Biology *29*.19, 3216–3228.e9.

Zhou, C., Franconville, R., Vaughan, A.G., Robinett, C.C., Jayaraman, V., and Baker, B.S. (2015). Central neural circuitry mediating courtship song perception in male Drosophila. eLife *4*. M. Ramaswami, ed., e08477.

DECLARATION

Herewith I declare, that I prepared the doctoral dissertation
Context, circuit and modulation of courtship signal selection in *Drosophila*
on my own and with no other sources and aids than quoted.

Göttingen, December 2022

Elsa Steinfath